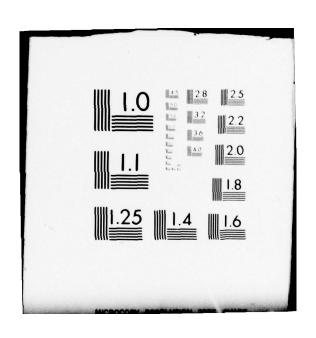
GTE SYLVANIA INC NEEDHAM HEIGHTS MASS ELECTRONIC SYS-ETC F/G 17/2 SUBBAND CODER STUDY. (U)
JUL 79 R S CHEUNG, R L WINSLOW DCA100-79-C-0001 AD-A074 427 DCA100-79-C-0001 SBIE-AD-E100 278 UNCLASSIFIED NL 1 of 2 AD A074427



MA074427



FINAL REPORT

SUBBAND CODER STUDY DCA 100-79-C-0001

THIS REPORT HAS BEEN PREPARED BY:

RONALD S. CHEUNG
RAIMOND L. WINSLOW

JULY 2, 1979





ELECTRONIC SYSTEMS GROUP EASTERN DIVISION

77 "A" STREET
NEEDHAM HEIGHTS, MASSACHUSETTS 02194

DISTRIBUTION STATEMENT A

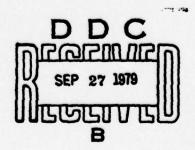
Approved for public release; Distribution Unlimited FINAL REPORT
SUBBAND CODER STUDY
DCA 100-79-C-0001

This report has been prepared by:

Ronald S. Cheung

Raimond L. Winslow

July 2, 1979



Unclassified		
Security Classification		
DOCUMENT CON (Security classification of title, body of abstract and indexin	TROL DATA - R & D	e overall report is classified)
GTE Sylvania 77 "A" Street Needham, MA 02194	26. REPORT S	Unclassified
Subband Coder Study,	12 12	8 7
Final Report	406 451	
2 July 79	76. TOTAL NO. OF PAGES 125 96. ORIGINATOR'S REPORT NU	76. NO. OF REFS 16 MBER(5)
(15) DCA 100-79-C-0001 July 27	6. OTHER REPORT NO(5) (Any this report)	other numbers that may be assigned
1. (19)AD-ETDE 21	none _	
10. DISTRIBUTION STATEMENT		DISTRIBUTION STATEMEN
Distribution of this document		Approved for public rele Distribution Unlimited
18 SBIE	Defense Comm 1860 Wiehle Reston, VA 1	unications Agency Avenue
This report gives a detain implementation of a speech was subband coders whose operation of the input speech band into of subbands individually. Be and the quadrature mirror fill studied and the result indicative yields much improved speech of former one.	veform coding te tions include the subbands and the oth the integer-be tering (QMF) app ites that the lat	chnique known e partitioning e quantization and sampling roaches are ter method
In addition to the design subband quantizers, practical of subband coders are considerate.	aspects in the	implementation
(1) a more efficient digit (2) a high speed multipli	tal interpolatio er-accumulator	n scheme, and

406 454

xll

Unclassified Security Classification KEY WORDS ROLE ROLE ROLE Subband Coding Integer-band Sampling Technique Digital Decimation Digital Interpolation Quadrature Mirror Filters Adaptive Bit Allocations Robust Quantizers Multiplier-Accumulator ACCESSION for NTIS White Section Buff Section DDC UNANNOUNCED JUSTIFICATION . DISTRIBUTION/AVAILABILITY CODES

Dist. AVAIL. and/or SPECIAL

Unclassified

AGO SISSA

Security Classification

13

TABLE OF CONTENTS

SECTION	TABLE OF CONTENTS	PAGE
	LIST OF ILLUSTRATIONS	iv
	LIST OF TABLES	vi
I	SUMMARY	
	1.1 Summary of the Program	1- 1
II	SOFTWARE SIMULATIONS	
	2.1 Introduction2.2 Operating Principles of Subband Coders	2- 1 2- 1
	2.2.1 Integer-band Sampling 2.2.2 Characteristics of Bandpass Filters	2- 3 2- 7
	2.2.3 Encoding of Subband Signals	2-12
	2.3 Practical Considerations in the Implementation of Subband Coders	2-14
	 2.3.1 Decimation Filtering 2.3.2 Interpolation Filtering 2.3.3 A Novel Technique in Digital Interpolation 	2-15 2-16 2-19
	2.4 Alternative Subband Coding Techniques	2-28
	2.4.1 Recursive Filter Approach 2.4.2 Quadrature Mirror Filter Approach	2-28 2-30
	2.4.2.1 Subband Coding via OMF Filter	2-34
	2.4.2.2 Adaptive Bit Alloca- tions	2-38
	2.4.2.3 Discussion of Results	2-41
III	THE MULTIPLIER-ACCUMULATOR HARDWARE	3- 1
	3.1 General Description3.2 Programming Considerations	3- 1 3- 3
IV	REAL-TIME SOFTWARE	4- 1
	4.1 Introduction 4.2 Speech/Line Side Interrupt 4.3 Initialization and Wait Loop 4.4 Transmitter/Receiver Synchronization 4.5 Decimation Filtering 4.6 Quantization and Encoding 4.7 Decoding and Dequantization 4.8 Interpolation Filtering 4.9 Operating Procedures of the Real-Time Subband Coder Programs	4- 1 4- 2 4- 6 4- 6 4-10 4-14 4-14 4-19
	4.9.1 9.6 Kb/s Program 4.9.2 16.0 Kb/s Program	4-24 4-25

'TABLE OF CONTENTS (CONT'D)

SECTION			PAGE
v	CONC	CLUSIONS AND RECOMMENDATIONS	5- 1
		Conclusions Recommendations	5- 1 5- 1
	REFE	ERENCES	5- 3
	APPENDIC	res	
	Α.	FILTER COEFFICIENTS OF 9.6 KB/S SUBBAND CODER	A- 1
		A.1 Band 1 A.2 Band 2 A.3 Band 3 A.4 Band 4	A- 1 A- 3 A- 5 A- 7
	В.	FILTER COEFFICIENTS OF 16.0 KB/S SUBBAND CODER	B- 1
		B.1 Band 1 B.2 Band 2 B.3 Band 3 B.4 Band 4 B.5 Band 5	B- 1 B- 3 B- 5 B- 7 B- 9
	c.	TABULATION OF THE 60-TAP QMF IMPULSE RESPONSE	
	D.	ROBUST QUANTIZER	D- 1
	Е.	EVALUATING TRANSCENDENTAL FUNCTIONS WITHOUT DIVISION	E- 1

1

LIST OF ILLUSTRATIONS

FIGURE		PAGE
2- 1	Block Diagram of the Subband Coder	2- 2
2- 2	Integer-band Sampling and a Frequency Domain Interpretation	2- 4
2- 3	Spectral Response of 9.6 Kb/s System	2-10
2- 4	System Response of 16 Kb/s Subband Coder	2-11
2- 5	Quantizer Characteristics	2-13
2- 6	Decimation Filter Structure (N Even)	2-17
2- 7	Filter Structure for the Novel Interpolation Scheme	2-26
2- 8	Band-Splitting and Reconstruction Using Single Stage QMF	2-31
2- 9	Magnitude Response of the 60-tap QMF Filter	2-35
2-10	Transmitter and Receiver of QMF Subband Coder	2-36
2-11	Spectral Response of 60-tap QMF Subband Coder	2-43
2-12	A Plot of Signal-to-Noise Ratio in DB versus Frame Number for the 9.6 Kb/s QMF Subband Coder (Cumulative SNR = 15.90 dB)	2-45
2-13	A Plot of Signal-to-Noise Ratio in dB versus Frame Number for the 16 Kb/s QMF Subband Coder (Cumulative SNR = 21.37 dB)	2-46
3- 1	Block Diagram of the High Speed Multiplier-Accumulator	3- 2
3- 2	A PSP Program to Demonstrate the Utility of MULACC	3-10
4- 1	Flow Chart of Speech Side Interrupt Service Routine	4- 3
4- 2	Flow Chart of Line Side Interrupt Service Routine	4- 4
4- 3	Storage of Filter Coefficients in MULACC	4- 7
4- 4	Flow Chart of the Wait Loop	4- 8
4- 5	Flow Chart of the Synchronization Routine	4- 9
4- 6	Loading of the Y-Buffer for Decimation Filtering	4-11
4- 7	Flow Chart of Decimation Filtering	4-13
4- 8	Flow Chart of an 8-Level Robust Quantizer	4-15
4- 9	Flow Chart of the Encoder	4-16
4-10	Transmission Data Formats for 9.6 and 16.0	4-17

FIGURE		PAGE
4-11	Flow Chart of a "K"-Bit Decoder	4-18
4-12	Flow Chart of an 8-Level Robust Dequantizer	4-20
4-13	Flow Chart for Interpolation Filtering	4-21
4-14	Storage of X and Y-Buffers for Interpolated	4-23

I

I

I

1

I

1

-

100 701

1

1

1

1

1

LIST OF TABLES

I

TABLE		PAGE
2- 1	Specifications of 9.6 Kb/s Subband Coder	2- 8
2- 2	Specifications of 16.0 Kb/s Subband Coder	2- 9
2- 3	APCM Coder Parameters	2-14
2- 4	Number of Multiplies Per Frame For Digital Decimation	2-18
2- 5	Number of Multiplies Per Frame For Interpolation Filtering	2-20
2- 6	Number of Multiplies Per Frame For Digital Interpolation with New Technique	2-27
2- 7	Specifications of 9.6 and 16.0 Kb/s QMF Subband Coders	2-42
3- 1	MULACC Instructions	3- 4
3- 2	Multiplier Functions	3- 6
3- 3	Instructions to Read Buffer Memories and Multiplier Products	3- 7
3- 4	Notes on Programming the MULACC	3- 8

SECTION I Summary

1.1 Summary of the Program

Under the six-month Subband Coder Study Contract, (DCA 100-79-C-0001), GTE Sylvania developed real-time software for a full-duplex 9.6 Kb/s and a half-duplex 16.0 Kb/s speech transmission scheme using the subband encoding technique. This software was designed to operate on the two GTE Sylvania Programmable Signal Processors (PSP) already owned by the Defense Communications Agency.

This study and implementation effort has resulted in a number of significant accomplishments in developing speech processing algorithms and hardware. Among them, the most important ones are:

- the development of real-time software for the
 and 16.0 Kb/s subband coders
- 2) the development of a high speed programmable multiplier-accumulator (MULACC)
- 3) the development of a novel digital interpolation scheme
- 4) the development of an improved subband coder that employs quadrature mirror filters (QMF)

The Subband Coder Study was motivated by initial Bell Laboratories simulations which showed that the algorithm has potential of providing good performance with reasonable complexity at data rates between 9.6 and 16.0 Kb/s. Preliminary listening tests indicated that the subband coder yielded better speech quality than the continuously variable slope delta modulation (CVSD) of the same data rate. However, to evaluate the algorithm fully, a large number of processed sentences is necessary. Since it is impractical to generate such a data base using FORTRAN floating point simulations, real-time implementation of the subband coder algorithm on the PSP's provides a viable solution.

Though the subband coder is conceptually simple, programming of the algorithm on the PSP using fixed-point arithemtic is non-trivial based on the limitations of the machine's computational

speed and 16-bit accuracy. One such problem arises when the exact Bell Lab's band-pass filters have to be utilized in order to duplicate their simulations. These filters, in general, are characterized by their sharp cutoffs and flat passband responses. Unfortunately, each of them is 200 taps long and this increases tremendously the processing requirements. Furthermore, the fixed-point 16-bit arithmetic hardware in the PSP does not provide enough accuracy in performing the bandpass filtering operation due to intermediate product truncations and roundoffs. To circumvent the mentioned difficulties, GTE Sylvania designed a high-speed multiplier-accumulator (MULACC) which performs a 16 x 16 bit multiplication with a 35-bit product accumulation in 208 nsec (2 PSP machine cycles). Occupying two PC cards, this circuitry communicates to the PSP CPU via the I/O buses. One apparent advantage of the hardware is that the PSP's basic design remains unchanged and existing software is still operable on the modified machines. Moreover, the speed and accuracy of MULACC permits the real-time implementations of 9.6 and 16.0 Kb/s subband coders on the PSP's.

To further simplify the complexity of the algorithm, GTE Sylvania developed a new digital interpolation scheme which is capable of reducing the number of multiplications needed by 50%. Even though the method is not utilized in the real-time implementations, it can be directly applied to other signal processing areas that involve digital interpolations.

Upon the completion of the real-time programming, extensive listening tests were performed on the processed outputs. The results indicate that the speech quality of the subband coder is slightly "hollow" and noisy especially for the 9.6 Kb/s system, but its overall quality is significantly better than that of CVSD. However, when compared to other high quality 16 Kb/s speech encoding schemes, such as the Adaptive Predictive Coder with Adaptive Quantization (APCQ) developed for DCA under Contract DCA-100-76-C-0002, the subband coder is clearly inferior. This can be partly attributed to the fact that the four or five band-pass filters employed by the subband coder algorithm are not

adequate to represent the entire speech spectrum. This introduces spectral "gaps" which manifest the "hollowness" in the processed speech. Moreover, the ratio of subband energies fluctuates largely from frame to frame and quantization of them using adaptive PCM (APCM) with fixed bit allocations is suboptimal.

Armed with this new information, GTE Sylvania developed a FORTRAN simulation of an improved subband coding scheme using quadrature mirror filters (QMF). Utilizing a 3-stage QMF structure, the input speech band is split into 8 subbands which can be recombined perfectly to form the original one. No spectral distortions are introduced in the bandsplitting and reconstruction processes even with a relatively short filter. Furthermore, to enable a more efficient encoding of the subband waveforms, an adaptive bit allocation scheme is incorporated which assigns different quantizer bits according to the energies of the subbands. As compared to the original subband coder, FORTRAN simulations of the QMF approach indicate that the processed speech is much improved and especially at 16 Kb/s, high quality speech is resulted.

Because of the improved voice quality provided by the QMF subband coder, further work should be performed to refine the algorithm and implement it in real-time on the modified PSP's.

SECTION II

SOFTWARE SIMULATIONS

2.1 Introduction

I

I

I

The subband coding algorithms investigated under this contract are generally classified as waveform coding techniques which, in contrast to source encoding methods that model only the sources of speech production, utilize speech waveform properties, such as, distributions of amplitude and power, nonflat characteristics of speech spectra. Moreover, though quantization is applied to actual time waveforms, subband coding is categorized as a frequency domain technique [1]. This is due to the fact that the input speech band is partitioned into several frequency components known as subbands and they are individually encoded. By varying dynamically the number of bits utilized to quantize each subband, the overall available bits can be distributed such that the important frequency component is quantized with more accuracy. In the case of speech signals, perceptually important acoustic attributes, such as pitch and first formant which are located at low frequency subbands, are preferentially encoded with more bits. However, for upper subbands where fricatives or unvoiced sounds occur, encoders with fewer bits/sample are utilized since these subbands contribute less perceptually. An obvious advantage of subband coding over coding in full band is that different quantizers are employed. As a result, the quantization noise is confined to each individual subband and this prevents the masking of signals in one frequency band by quantization noise of another.

2.2 Operating Principles of Subband Coder

Operations of the subband coder include the partitioning of the input speech band into N subbands using bandpass filters, H_1 , H_2 , ... H_N in the manner shown in Figure 2-1. Each of the resulting

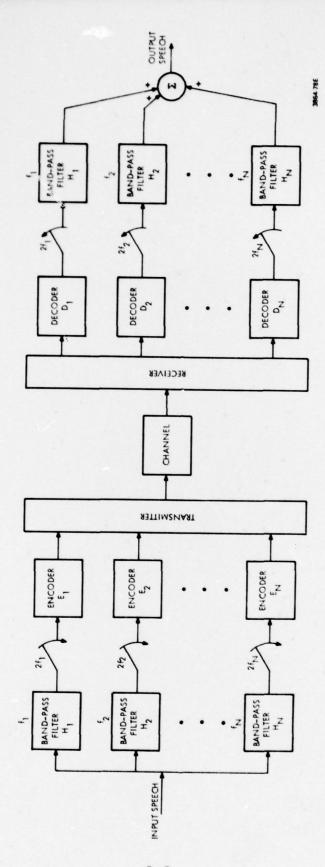


FIGURE 2-1 BLOCK DIAGRAM OF THE SUBBAND CODER

subbands, after frequency translation to DC, is digitally encoded for transmission. At the receiver, these transmitted data are decoded and later modulated upwards to their corresponding center frequencies. After bandpass filtering, the resulting subbands are then added together to form an estimate of the input signal [2].

2.2.1 Integer-Band Sampling

To perform the frequency translations of the subband spectra, generally a complicated modulation/demodulation scheme has to be applied. Fortunately, through a new technique known as integer-band sampling, this modulation process can be avoided [3]. This method calls for the filtering of the input signal into subbands of bandwidths W₁ followed by the resampling of the outputs at their corresponding Nyquist rates 2W₁. At the receiver, the reverse operation is performed which reconstructs the input waveform through upsampling the decoded subbands followed by bandpass filtering. Though the integerband sampling technique alleviates the use of any complex modulation schemes, the choice of subbands is rather restricted. Moreover, to prevent spectral aliasing, the subbands have to lie between frequencies kW₁ and (k+1)W₁ where k is an integer.

For explanatory purposes, the bandpass filtering of one subband is detailed in Figure 2-2(a). If y(n) denotes the bandpass signal sampled originally at $f_s = \frac{1}{T}$, and $Y(e^{jWT})$, the spectrum of y(n), is depicted in Figure 2-2(b). The resampled signal $y_1(n)$ is given by:

$$y_1(n) = y(Mn) = y\left(\frac{f_s}{2W_1}n\right)$$
 (2-1)

where $M = \frac{f_s}{2W_i}$ is defined as the decimation ratio. Consequently, $y_1(n)$ has a lower sampling rate $f_s' = \frac{1}{T\ell} = \frac{f_s}{M}$.

Defining a new sequence w(n) as:

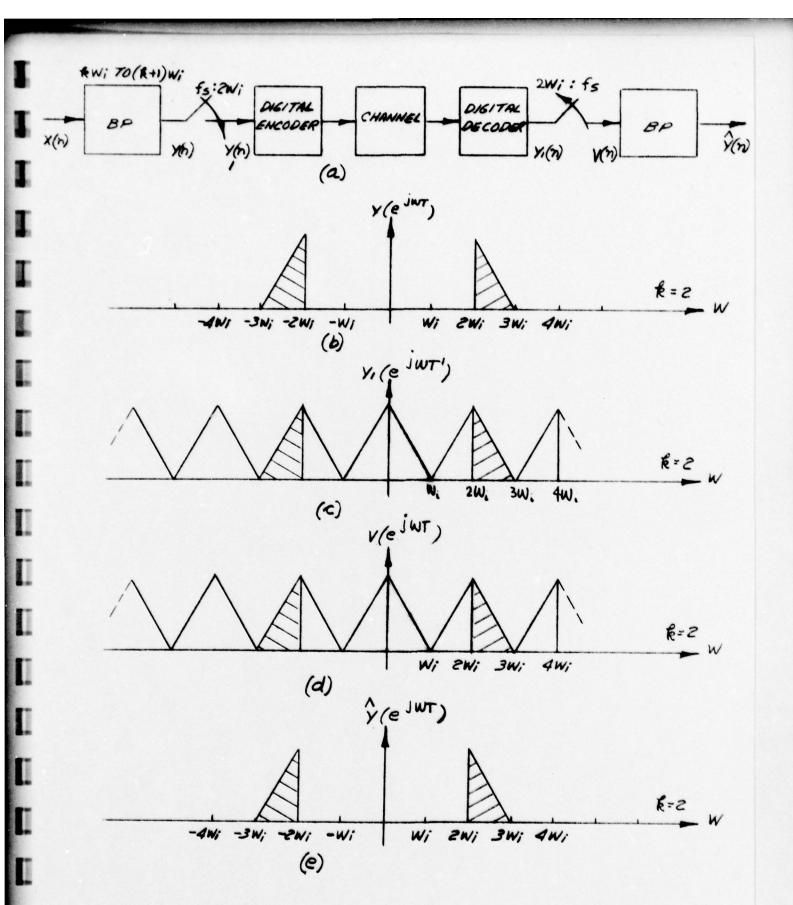


FIGURE 2-2 INTEGER-BAND SAMPLING AND A FREQUENCY
DOMAIN INTERPRETATION
2-4

$$w(n) = \begin{cases} y(n) & \text{if } n=0, \pm M, \pm 2M, \dots \\ 0 & \text{otherwise} \end{cases}$$
 (2-2)

or
$$w(n) = \frac{y(n)}{M} \sum_{k=0}^{M-1} e^{j \frac{2\pi k n}{M}}$$
 (2-3)

The sequence $y_1(n)$ can be rewritten as:

$$y_1(n) = w(Mn) \tag{2-4}$$

To compare the spectra of $y_1(n)$ and y(n), the Z-transform of Eq. (2-4) is taken which yields [4]:

$$Y_{1}(Z) = \sum_{n=-\infty}^{\infty} w(Mn) Z^{-n}$$

$$= \sum_{n=-\infty}^{\infty} w(n) \overline{Z}^{n/M}$$

$$= \frac{1}{M} \sum_{\ell=0}^{M-1} \left(\sum_{n=-\infty}^{\infty} y(n) e^{j \frac{2\pi \ell n}{M}} Z^{-n/M} \right)$$

$$= \frac{1}{M} \sum_{\ell=0}^{M-1} Y\left(e^{-j \frac{2\pi \ell}{M}} Z^{1/M} \right)$$
(2-5)

The Fourier transform is obtained by evaluating the Z-transform shown in Eq. (2-5) on the unit circle and this results in:

$$Y_1(e^{jwT'}) = \frac{1}{M} \sum_{k=0}^{M-1} Y(e^{j(wT'-2\pi k)/M})$$
 (2-6)

From Eq. (2-6), Y₁(e^{jwT'}) depicts a repeated version of Y(e^{jwT'}) and a graphical representation of it is shown in Figure 2-2(c). To prevent spectral aliasing, it is clear that the subband frequency has to lie between kW₁ and (k+1)W₁ where k is an integer (k=2 in Figure 2-2). This imposes a constraint on the choice of subbands which affects the performance of subband coders tremendously.

At the receiver, the decimated signal $y_1(n)$ is interpolated upwards M times in order to achieve the original sampling frequency of $f_s = \frac{1}{T}$. In fact, every (M-1) zeros are inserted between consecutive y(n)'s and the resulting sequence v(n) is defined as:

$$v(n) = \begin{cases} y_1(n/M) & \text{if } n=0, \pm M, \pm 2M, \dots \\ \phi & \text{otherwise} \end{cases}$$
 (2-7)

To see the relationships between the spectra of v(n) and $y_1(n)$, take the Z-transform of v(n) and this yields:

$$V(Z) = \sum_{n=-\infty}^{\infty} y_1(n/M) Z^{-n} = \sum_{n=-\infty}^{\infty} y_1(n) Z^{-Mn}$$

$$= Y_1(Z^{m})$$
(2-8)

The Fourier transform of Eq. (2-8) is:

$$V(e^{jwT}) = Y_1(e^{jwTM}) = Y_1(e^{jwT'})$$
(2-9)

where T' is the sampling period of the decimated waveform $y_1(n)$. A graphical representation of $V(e^{\mathbf{j}wT})$ is shown in Figure 2-2(d).

From Eq. (2-9), the spectrum of v(n) has the identical shape as that of $y_1(n)$ after normalization with respect to their sampling rates. By bandpass filtering v(n), a replica of y(n) is created as shown in Figure 2-2(e).

2.2.2 Characteristics of Band Pass Filters

Utilizing the integer-band sampling technique, the dividing of input speech band into subbands is accomplished with a set of bandpass filters whose passbands are chosen to span the entire speech band with minimal overlap. Specifications of 9.6 and 16.0 Kb/s subband filters and quantizer parameters are summarized in Tables2-1 and 2-2. For the 9.6 Kb/s system, there are four subbands which cover ranges from 240-2880 Hz. Each of the filters is 200 taps long and is characterized by a relatively flat pass-The coefficients of the bandband and a short transition region. pass filters, furnished by R. Crochiere of Bell Labs, are shown in Appendix A. The overall magnitude response of the 9.6 Kb/s system, obtained by combining the responses of the 4 filters, is shown in Figure 2-3 and it reveals large spectral gaps at frequencies around 1000 Hz and 1800 Hz which accounts for the "hollow" and reverberent quality in the processed speech. As for the 16.0 Kb/s system, five subbands which span frequencies from 178-3200 Hz are utilized. These filters are also 200 taps long and their coefficients are tabulated in Appendix B. The overall magnitude response, obtained by combining the responses of five filters, is shown in Figure 2-4. As compared to that of the 9.6 Kb/s system, Figure 2-4 shows a narrowing of the gaps in the reconstructed spectrum which results in improved speech quality.

Sampling Rate = 9.6 KHz

Data Rate = 9.6 Kb/s

No. of Input Samples/Frame = 180

Frame Time = 18.75 msec

SUBBAND NO.	BAND EDGES (HZ)	DECIMATION (INTERPOLATION) RATIO	NO. OF DECIMATED SAMPLES/FRAME	QUANTIZER BITS	NO. OF SUBBAND BITS/FRAME	MIN STEP SIZE AMIN	MAX STEP SIZE AMAX	STEP SIZE THRESHOLD ATH
1	240- 480	20	6	3	27	5	1280	5
5	096 -081	10	18	2	36	9	1536	9
3	1067-1600	6	20	2	04	9	1536	9
4	1920-2880	5	36	2	72	7	1792	7
Synchronization					5			
TOTAL					180			

TABLE 2-1 SPECIFICATIONS OF 9.6 KB/S SUBBAND CODER

Sampling Rate = 10.6667 KHz Data Rate = 16.0 KB/s

III

Special S

П

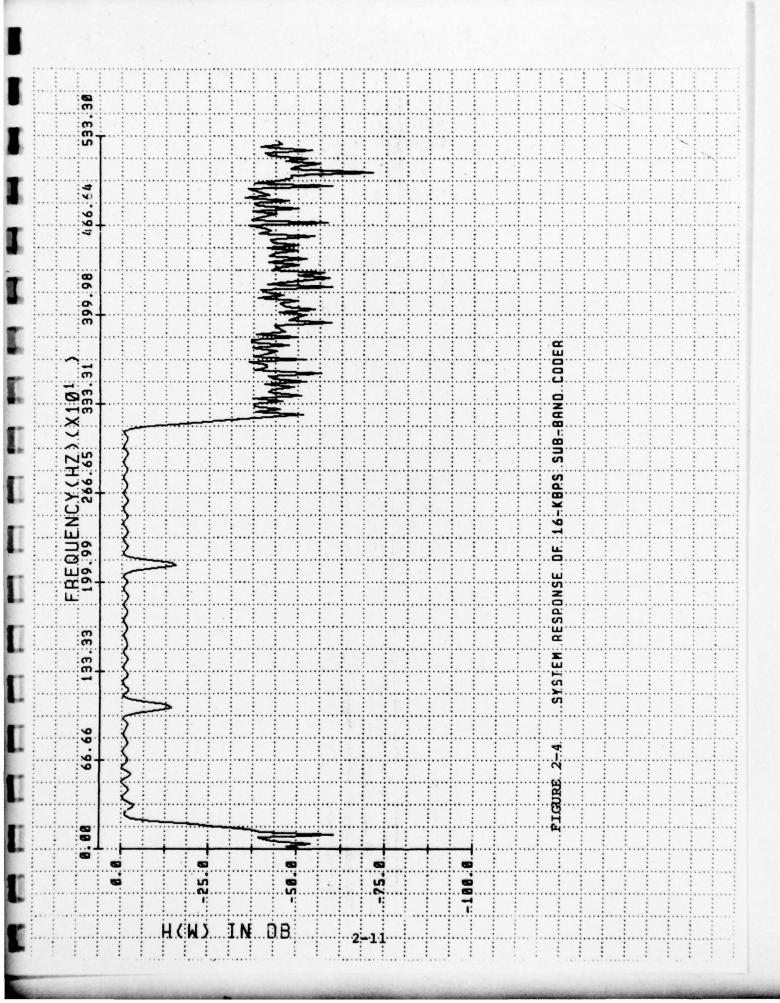
I

No. of Input Samples/Frame = 90

Frame Time = 8.4375 msec

SUBBAND NO.	BAND EDGES (HZ)	DECIMATION (INTERPOLATION) RATIO	NO. OF DECIMATED SAMPLES/FRAME	QUANTIZER BITS	NO. OF SUBBAND BITS/FRAME	MIN STEP SIZE AMIN	MAX STEP SIZE AMAX	STEP SIZE THRESHOLD ATH
1	178- 356	30	3	7	12	5	1280	0
8	296- 593	18	5	7	20	5	1280	0
3	533-1067	10	6	3	27	9	1536	0
4	1067-2133	5	18	5	36	9	1536	7
5	2133-3200	5	18	2	36	7	1792	7
Synchronization					7			
TOTAL					135			
						The state of the s		

TABLE 2-2 SPECIFICATIONS OF 16.0 KB/S SUBBAND CODER

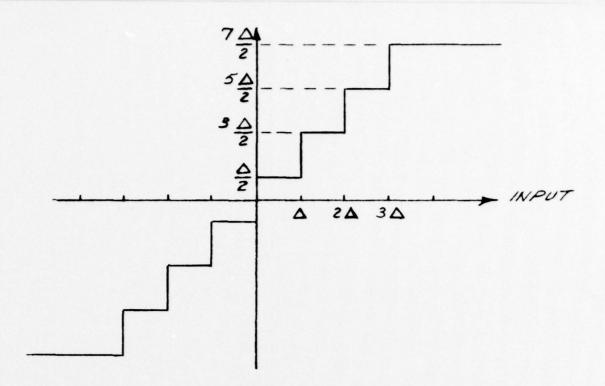


2.2.3 Encoding of Subband Signals

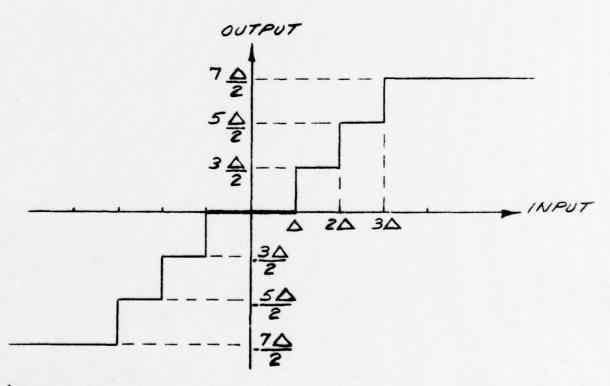
It is well known that the long-term spectrum of speech signals tends to decrease in power density with frequency, yet the drop is relatively small for waveforms across any one subband. In other words, after frequency translation of the bandpassed input to DC and resampling it at the Nyquist rate, the signal has little correlation between adjacent samples and encoding of it was shown to be best performed using adaptive PCM (APCM) [3]. The most common scheme is the stepsize adaptation strategy which utilizes one-word step size This technique is dealt with in great depth in recent literature and it will not be treated in detail here. Basically, a B-bit quantizer (where B is an integer) is employed to encode the input sample into one of the possible Then the quantizer updates its step size after every input sample. In general, these quantizers are referred to as mid-rise quantizers and an example is a 3-bit quantizer whose characteristic is shown in Figure 2-5(a). Also, multiplication factors for 2, 3, and 4-bit quantizers are listed in Table 2-3.

In practice, minimum (Δ min) and maximum (Δ max) values have to be imposed on the step sizes to assure proper quantizer adaptation. Hence, an obvious disadvantage of mid-rise quantizers is that it cannot represent a zero level. For small amplitude inputs, the quantized values always oscillate between $\pm\Delta$ min which are perceived as a low level tone. In the case of subband coders, this low level tone will be frequency translated back in the middle of the speech band where they are particularly noticeable. Hence, even with a small Δ min, the distortion is still very disturbing.

One method to alleviate the low volume tones is to make use of the mid-tread quantizer. An example is the 7-level quantizer whose characteristic is shown in Figure 2-5(b). Since the quantizer has a zeroth step, all low level



(2) THE 8-LEVEL MID-RISE QUANTIZER CHARACTERISTIC



(b) THE 7-LEVEL MID-TREAD QUANTIZER CHARACTERISTIC

inputs are then coded to be zero and this eliminates the tones. Hence, mid-tread quantizers seem advantageous for subband coders. However, in contrast to a mid-rise one, a B-bit midtread quantizer has less than 2^B levels and this represents a decrease in coding efficiency. For subband coders, tread quantizers can still be employed without losing much efficiency. This is accomplished by utilizing a mid-rise/midtread dequantizer switch at the receiver. In this case, the transmitter employs conventional B-bit mid-rise quantizers whereas the receiver can select either mid-tread or mid-rise to dequantize the data. As a matter of fact, a step-size threshold value (Ath) is setup in such a way that a mid-tread dequantizer is selected if $\Delta < \Delta$ th whereas the mid-rise dequantizer is utilized for $\Delta > \Delta th$. Threshold values for the 9.6 and 16.0 Kb/s subband coders are experimentally determined and they are included in Tables 2-1 and 2-2.

STEP SIZE MULTIPLICATION	QUANTIZER BITS		
FACTOR	4	3	2
М 1	0.9	0.85	0.85
М 2	0.9	1.0	1.9
М з	0.9	1.0	
M 4	0.9	1.5	
М 5	1.2		
М 6	1.6		
Му	2.0		
Мв	2.4		

TABLE 2-3 APCM CODER PARAMETERS

2.3 Practical Considerations in the Implementation of Subband Coders

The subband coders as discussed in Section 2.2 employ a bank of 4 or 5 FIR filters to perform bandpass filtering. One

obvious advantage is due to the linearity of the FIR filter's phase response with respect to frequency which eliminates distortions introduced by time delays of different subbands. However, to achieve the desired bandpass characteristics, length of FIR filters is generally long (e.g., 200 taps) thus increasing the processing requirements. In the real-time implementations of subband coders, the success is greatly dependent on the efficient programming of the bandpass filtering operation and the following sections consider in more detail the number of mathematical operations (in particular, the number of multiplies) required.

2.3.1 Decimation Filtering

The outputs of a bandpass filter is given by the convolution-sum

$$y(n) = \sum_{k=0}^{N-1} h(k)x(n-k)$$
 (2-10)

where N is the order of the filter, h(k) is the k^{th} filter coefficient, and x(n), y(n) represent the input, output sample, respectively. It is clear from Eq. (2-10) that N multiplications are needed to compute each y(n). However, the integer-band sampling technique calls for the down-sampling of the filtered output to obtain $y_1(n)$. In other words, only every M^{th} point has to be calculated where M is the decimation ratio and Eq. (2-10) can be re-written as:

$$y_1(n) = y(Mn) = \sum_{k=0}^{N-1} h(k)x(Mn-k)$$
 (2-11)

Henceforth, the total number of multiplies required for each input sample becomes N/M. Furthermore, since the impulse response of a FIR filter satisfies:

$$h(n) = h(N-1-n)$$
 (2-12)

Eq. (2-11) can be shown as (for N even):

$$y_1(n) = y(Mn) = \sum_{k=0}^{\frac{N}{2}-1} h(k) \left(x(Mn-k) + x(Mn-N+k+1) \right)$$
 (2-13)

Then the symmetry of the filter reduces the number of multiplies by 50% (or N/2M per input sample). The above derivation can also be applied to the case when N is odd. Figure 2-6 illustrates the structure that exploits the symmetry property of the FIR filters. Table 2-4 summarizes the number of multiplies needed for each band to perform decimation filtering in the 9.6 and 16.0 Kb/s subband coders.

2.3.2 Interpolation Filtering

There are a number of methods which may be used to perform interpolation filtering. The most straightforward method is to pad in (M-1) zeros between each decimated sample value where M in this case the interpolation ratio, and bandpass filter the resulting sequence. Using this technique, the filter structure as shown in Figure 2-6 is also capable of performing interpolation filtering. Though the symmetry of linear phase FIR filters can be employed to decrease the number of multiplies, the amount of multiplications required (N/2 per input sample) is still excessive. However, cognizant of the fact that there are no multiplications involved with samples of zero values, this number can be greatly reduced. Referring to Figure 2-2(a), the synthesized sample $\hat{y}(n)$ is shown as

$$\hat{y}(n) = \sum_{k=0}^{N-1} h(k)y(n-k)$$
 (2-14)

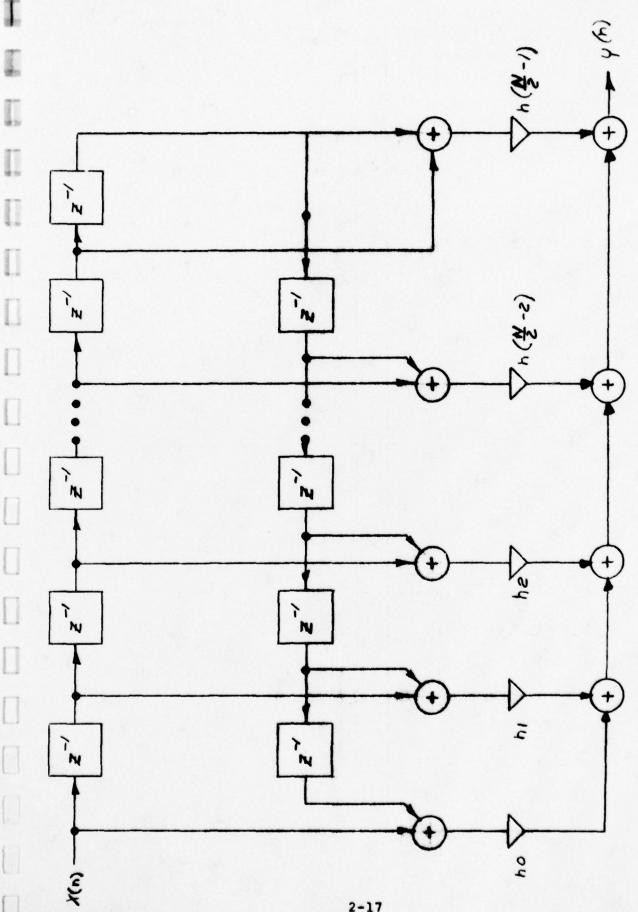


FIG 2-6 DECIMATION FILTER STRUCTURE (NEVEN)

2-17

SUBBAND #	# OF MULTIPLIES PER FRAME IN 9.6 KB/S SYSTEM	# OF MULTIPLIES PER FRAME IN 16.0 KB/S SYSTEM
1	900	300
2	1800	500
3	2000	900
4	3600	1800
5		1800
TOTAL	8300	5300

TABLE 2-4 NUMBER OF MULTIPLIES PER FRAME FOR DIGITAL DECIMATION

Substituting Eq. (2-7) into (2-14), $\hat{y}(n)$ can be rewritten as

$$\hat{y}(n) = \sum_{k=0}^{N-1} h(k) y_1 \left[\frac{n-k}{M} \right]$$
 (2-15)

where

$$\begin{bmatrix} \xi \end{bmatrix} = \begin{cases} \xi; & \text{if } \xi \text{ is an integer} \\ 0; & \text{otherwise} \end{cases}$$
 (2-16)

Using this technique, the number of multiplies required per input sample as shown in Eq. (2-15) is equal to the integer quotient {N/M}. The total number of multiplies per frame for interpolation filtering in the subband coders is shown in Table 2-5.

2.3.3 A Novel Technique in Digital Interpolation

If Table 2-5 is compared to Table 2-4, it is shown that the interpolation filtering requires twice the number of multiplies as that of decimation filtering. This can be attributed to the fact that the symmetry of FIR filters cannot be exploited in the interpolation case [4]. However, by rearranging and combining some of the input samples, the symmetry of the filter can indeed be employed to reduce the total number of multiplies at the expense of more additions (subtractions).

Defining

$$m = \left\{\frac{N-1}{M}\right\} \tag{2-17}$$

where $\{\cdot\}$ is the integer quotient, N is the filter length and M is the decimation ratio, the remainder α can be written as:

$$\alpha = N-1 - mM \tag{2-18}$$

# OF MULTIPLIES PER FRAME REQUIRED IN 9.6 KB/S SYSTEM	# OF MULTIPLIES PER FRAME REQUIRED IN 16.0 KB/S SYSTEM
1,800	630
3,600	1,080
4,000	1,800
7,200	3,600
	3,600
16,600	10,710
	PER FRAME REQUIRED IN 9.6 KB/S SYSTEM 1,800 3,600 4,000 7,200

I

I

I.

TABLE 2-5 NUMBER OF MULTIPLIES PER FRAME FOR INTERPOLATION FILTERING

Then Eq. (2-15), for the first M samples, can be expanded as:

$$\hat{y}(0) = \hat{h}(0) y_i(0) + \hat{h}(M) y_i(-i) + \cdots + \hat{h}(mM-M) y_i(-m+i) + \hat{h}(mM) y_i(-m)$$

$$\hat{y}(1) = \hat{h}(1) y_i(0) + \hat{h}(M+1) y_i(-i) + \cdots + \hat{h}(mM-M+1) y_i(-m+1) + \hat{h}(mM+1) y_i(-m)$$

Making use of the symmetry of h(n) as defined in Eq. (2-12),

$$f_{(mM)} = f_{(a)}$$

$$f_{(mM-m)} = f_{(a+m)}$$

$$\vdots$$

$$f_{(0)} = f_{(N-1)}$$

$$(2-20)$$

Substituting Eq. (2-20) into (2-19), the following equations are resulted:

$$\frac{1}{3}(0) = \frac{1}{3}(0)\frac{1}{3}(0) + \frac{1}{3}(0)\frac{1}{3}(-1) + \cdots + \frac{1}{3}(\frac{1}{3}(-m+1)) + \frac{1}{3}(\frac{1}{3}(-m)) \\
\frac{1}{3}(1) = \frac{1}{3}(1)\frac{1}{3}(0) + \frac{1}{3}(\frac{1}{3}(-1)) + \cdots + \frac{1}{3}(\frac{1}{3}(-m+1)) + \frac{1}{3}(\frac{1}{3}(-m)) \\
\frac{1}{3}(\frac{1}{3}(-m+1))\frac{1}{3}(0) + \frac{1}{3}(\frac{1}{3}(-m+1)) + \cdots + \frac{1}{3}(\frac{1}{3}(-m+1)) + \cdots + \frac{1}{3}(\frac{1}{3}(-m+1)) \\
\frac{1}{3}(\frac{1}{3}(-m+1))\frac{1}{3}(0) + \frac{1}{3}(\frac{1}{3}(-m+1))\frac{1}{3}(-m+1) + \cdots + \frac{1}{3}(\frac{1}{3}(-m+1)) \\
\frac{1}{3}(\frac{1}{3}(-m+1))\frac{1}{3}(0) + \frac{1}{3}(\frac{1}{3}(-m+1))\frac{1}{3}(-m+1) + \cdots + \frac{1}{3}(\frac{1}{3}(-m+1))\frac{1}{3}(-m+1)$$

$$\vdots \\
\frac{1}{3}(\frac{1}{3}(-m+1))\frac{1}{3}(0) + \frac{1}{3}(\frac{1}{3}(-m+1))\frac{1}{3}(-1) + \cdots + \frac{1}{3}(\frac{1}{3}(-m+1))\frac{1}{3}(-m+1)$$

$$\vdots \\
\frac{1}{3}(\frac{1}{3}(-m+1))\frac{1}{3}(0) + \frac{1}{3}(\frac{1}{3}(-m+1))\frac{1}{3}(-1) + \cdots + \frac{1}{3}(\frac{1}{3}(-m+1))\frac{1}{3}(-m+1)$$

I

I

B 100 B

No.

Total St.

I

A closer examination of Eq. (2-21) reveals great similarity between sample pairs $\hat{y}(0)$ and $\hat{y}(\alpha)$; $\hat{y}(1)$ and $\hat{y}(\alpha-1)$... In other words, if they are combined, the following is true:

$$\begin{cases} Q_{0} \stackrel{\triangle}{=} \frac{1}{2} (\mathring{g}(0) + \mathring{g}(\omega)) = \frac{(h(0) + h(\omega))}{2} (\mathring{g}_{1}(0) + \mathring{g}_{1}(-m)) + (\frac{h(m) + h(m+\omega)}{2}) (\mathring{g}_{1}(-1) + \mathring{g}_{1}(-m+1)) + \dots \\ h_{0} \stackrel{\triangle}{=} \frac{1}{2} (\mathring{g}(0) - \mathring{g}(\omega)) = \frac{(h(0) - h(\omega))}{2} (\mathring{g}_{1}(0) - \mathring{g}_{1}(-m)) + (\frac{h(m) - h(m+\omega)}{2}) (\mathring{g}_{1}(-1) - \mathring{g}_{1}(-m+1)) + \dots \\ Q_{1} \stackrel{\triangle}{=} \frac{1}{2} (\mathring{g}(1) + \mathring{g}(\omega-1)) = (\frac{h(1) + h(\omega-1)}{2}) (\mathring{g}_{1}(0) + \mathring{g}_{1}(-m)) + (\frac{h(m+1) + h(m+\omega-1)}{2}) (\mathring{g}_{1}(-1) + \mathring{g}_{1}(-m+1)) + \dots \\ h_{1} \stackrel{\triangle}{=} \frac{1}{2} (\mathring{g}(1) - \mathring{g}(\omega-1)) = \frac{(h(1) - h(\omega-1))}{2} (\mathring{g}_{1}(0) - \mathring{g}_{1}(-m)) + (\frac{h(m+1) - h(m+\omega-1)}{2}) (\mathring{g}_{1}(-1) - \mathring{g}_{1}(-m+1)) + \dots \end{cases}$$

$$\begin{array}{l}
\Omega_{\left\{\frac{d}{2}\right\}} \triangleq \frac{1}{2} \left(\hat{y} \left(\left\{\frac{d}{2}\right\} \right) + \hat{y} \left(d - \left\{\frac{d}{2}\right\} \right) \right) = \frac{\left(\hat{h} \left(\left\{\frac{d}{2}\right\} \right) + \hat{h} \left(d - \left\{\frac{d}{2}\right\} \right) \right)}{2} \left(y_{10} \right) + y_{1} \left(-m \right) + \dots \\
b_{\left\{\frac{d}{2}\right\}} \triangleq \frac{1}{2} \left(\hat{y} \left(\left\{\frac{d}{2}\right\} \right) - \hat{y} \left(d - \left\{\frac{d}{2}\right\} \right) \right) = \frac{\left(\hat{h} \left(\left\{\frac{d}{2}\right\} \right) - \hat{h} \left(d - \left\{\frac{d}{2}\right\} \right) \right)}{2} \left(y_{10} \right) - y_{1} \left(-m \right) + \dots
\end{array}$$

where $\left\{\frac{\alpha}{2}\right\}$ denotes the largest integer of $\frac{\alpha}{2}$. Hence from Eq. (2-22),

Since it only takes $\left\{\frac{N-1}{2M}\right\}$ +1 multiplies to obtain $\left\{\frac{a}{2M}\right\}$ or b_i , the total number of multiplies for each $\hat{y}(k)$ is also $\left\{\frac{N-1}{2M}\right\}$ +1 which is about half the number required by the conventional method as shown in Eq. (2-15). Similarly, $\hat{y}(\alpha+1)$, $\hat{y}(M-1)$; $\hat{y}(\alpha+2)$, $\hat{y}(M-2)$; ... can be combined in the same fashion yielding:

$$b_{\left\{\frac{1}{2}\right\}+1} \stackrel{\Delta}{=} \frac{1}{2} \left(\hat{y}_{(M+1)} - \hat{y}_{(M-1)} \right) = \left(\frac{h(M+1) - h(M-1)}{2} \left(y_{1}(0) - y_{1}(-M+1) \right) + \left(\frac{h(M+d+1) - h(2M-1)}{2} \right) \left(y_{1}(-1) - y_{1}(-M+2) \right) + \cdots$$

and

$$\frac{4}{3}(\alpha_{H}) = \alpha_{\{\frac{d}{2}\}+1} + b_{\{\frac{d}{2}\}+1}$$
(2-25)

g(M-1) = a { 2/+1 - b { 2/+1

As shown in Eq. (2-25), it takes $\left\{\frac{N-1}{2M}\right\}$ multiplies to compute each $\hat{y}(k)$ where $k=\alpha+1, \alpha+2, \ldots$ M-1 which is also half the number required by the conventional way. Then the total number of multiplies needed to compute all M points is given by

$$M_{M} = \left(\left\{ \frac{N-1}{2M} \right\} + 1 \right) (\alpha + 1) + \left\{ \frac{N-1}{2M} \right\} (M-1-\alpha)$$

$$= \left\{ \frac{N-1}{2M} \right\} M + (\alpha + 1)$$
(2-26)

As an example, the filter structure needed to compute a_0 , b_0 (or equivalently $\hat{y}(0)$, $\hat{y}(\alpha)$) is depicted in Figure 2-7. To compute a_1 , b_1 (or $\hat{y}(1)$, $\hat{y}(\alpha-1)$, the same filter structure with a different coefficient set can be utilized.

Furthermore, to compute a new block of output data, $\hat{y}(k)$'s can be expanded as:

$$\frac{3}{4}(m) = \frac{1}{6}(0)\frac{1}{3}(1) + \frac{1}{6}(m)\frac{1}{3}(0) + \frac{1}{6}(2m)\frac{1}{3}(1-1) + \dots + \frac{1}{6}(4+m)\frac{1}{3}(1-m+2) + \frac{1}{6}(4)\frac{1}{3}(1-m+1)}{3}(1-m+1)\frac{1}{3}(1-m+1)\frac{1}{3}(1-m+1)\frac{1}{3}(1-m+2) + \frac{1}{6}(4-1)\frac{1}{3}(1-m+1)\frac{1}{3}(1-m+1)\frac{1}{3}(1-m+1)\frac{1}{3}(1-m+1)\frac{1}{3}(1-m+1)\frac{1}{3}(1-m+1)\frac{1}{3}(1-m+1)\frac{1}{3}(1-m+1)\frac{1}{3}(1-m+1)\frac{1}{3}(1-m+1)\frac{1}{3}(1-m+1)\frac{1}{3}(1-m+1)\frac{1}{3}(1-m+1)\frac{1}{3}(1-m+1)\frac{1}{3}(1-m+1)\frac{1}{3}(1-m+1)\frac{1}{3}(1-m+1)\frac{1}{3}(1-m+1)\frac{1}{3}(1-m+1)\frac{1}{3}(1-m+1)\frac{1}{3}(1-m+1)\frac{1}{3}(1-m+1)\frac{1}{3}(1-m+1)\frac{1}{3}(1-m+1)\frac{1}{3}(1-m+1)\frac{1}{3}(1-m+1)\frac{1}{3}(1-m+1)\frac{1}{3}(1-m+1)\frac{1}{3}(1-m+1)\frac{1}{3}(1-m+1)\frac{1}{3}(1-m+1)\frac{1}{3}(1-m+1)\frac{1}{3}(1-m+1)\frac{1}{3}(1-m+1)\frac{1}{3}(1-m+1)\frac{1}{3}(1-m+1)\frac{1}{3}(1-m+1)\frac{1}{3}(1-m+1)\frac{1}{3}(1-m+1)\frac{1}{3}(1-m+1)\frac{1}{3}(1-m+1)\frac{1}{3}(1-m+1)\frac{1}{3}(1-m+1)\frac{1}{3}(1-m+1)\frac{1}{3}(1-m+1)\frac{1}{3}(1-m+1)\frac{1}{3}(1-m+1)\frac{1}{3}(1-m+1)\frac{1}{3}(1-m+1)\frac{1}{3}(1-m+1)\frac{1}{3}(1-m+1)\frac{1}{3}(1-m+1)\frac{1}{3}(1-m+1)\frac{1}{3}(1-m+1)\frac{1}{3}(1-m+1)\frac{1}{3}(1-m+1)\frac{1}{3}(1-m+1)\frac{1}{3}(1-m+1)\frac{1}{3}(1-m+1)\frac{1}{3}(1-m+1)\frac{1}{3}(1-m+1)\frac{1}{3}(1-m+1)\frac{1}{3}(1-m+1)\frac{1}{3}(1-m+1)\frac{1}{3}(1-m+1)\frac{1}{3}(1-m+1)\frac{1}{3}(1-m+1)\frac{1}{3}(1-m+1)\frac{1}{3}(1-m+1)\frac{1}{3}(1-m+1)\frac{1}{3}(1-m+1)\frac{1}{3}(1-m+1)\frac{1}{3}(1-m+1)\frac{1}{3}(1-m+1)\frac{1}{3}(1-m+1)\frac{1}{3}(1-m+1)\frac{1}{3}(1-m+1)\frac{1}{3}(1-m+1)\frac{1}{3}(1-m+1)\frac{1}{3}(1-m+1)\frac{1}{3}(1-m+1)\frac{1}{3}(1-m+1)\frac{1}{3}(1-m+1)\frac{1}{3}(1-m+1)\frac{1}{3}(1-m+1)\frac{1}{3}(1-m+1)\frac{1}{3}(1-m+1)\frac{1}{3}(1-m+1)\frac{1}{3}(1-m+1)\frac{1}{3}(1-m+1)\frac{1}{3}(1-m+1)\frac{1}{3}(1-m+1)\frac{1}{3}(1-m+1)\frac{1}{3}(1-m+1)\frac{1}{3}(1-m+1)\frac{1}{3}(1-m+1)\frac{1}{3}(1-m+1)\frac{1}{3}(1-m+1)\frac{1}{3}(1-m+1)\frac{1}{3}(1-m+1)\frac{1}{3}(1-m+1)\frac{1}{3}(1-m+1)\frac{1}{3}(1-m+1)\frac{1}{3}(1-m+1)\frac{1}{3}(1-m+1)\frac{1}{3}(1-m+1)\frac{1}{3}(1-m+1)\frac{1}{3}(1-m+1)\frac{1}{3}(1-m+1)\frac{1}{3}(1-m+1)\frac{1}{3}(1-m+1)\frac{1}{3}(1-m+1)\frac{1}{3}(1-m+1)\frac{1}{3}(1-m+1)\frac{1}{3}(1-m+1)\frac{1}{3}(1-m+1)\frac{1}{3}(1-m+1)\frac{1}{3}(1-m+1)\frac{1}{3}(1-m+1)\frac{1}{3}(1-m+1)\frac{1}{3}(1-m+1)\frac{1}{3}(1-m+1)\frac{1}{3}(1-m+1)\frac{1}{3}(1-m+1)\frac{1}{3}(1-m+1)\frac{1}{3}(1-m+1)\frac{1}{3}(1-m+1)\frac{1}{3}(1-m+1)\frac{1}{3}(1-m+1)\frac{1}{3}(1-m+1)\frac{1}{3}(1-m+1$$

I

I

1

I

I

By comparing Eqs. (2-27) with (2-19), it is clear that both sets are identical with the only exception that the input sequence is incremented by 1. Hence the filter structure as shown in Figure 2-7 can be used with the input y(1) to the filter. Repeating the above procedure, all interpolation outputs $\hat{y}(0)$, $\hat{y}(1)$, ... can be obtained. To show the efficiency of the new algorithm, the number of multiplications required for the 9.6 and 16.0 Kb/s subband coders, summarized in Table 2-6, shows that only half the number of multiplies is needed as compared to that of the conventional technique. Furthermore, utilizing this method, the muliplication necessary for both digital decimation and interpolation are roughly equivalent.

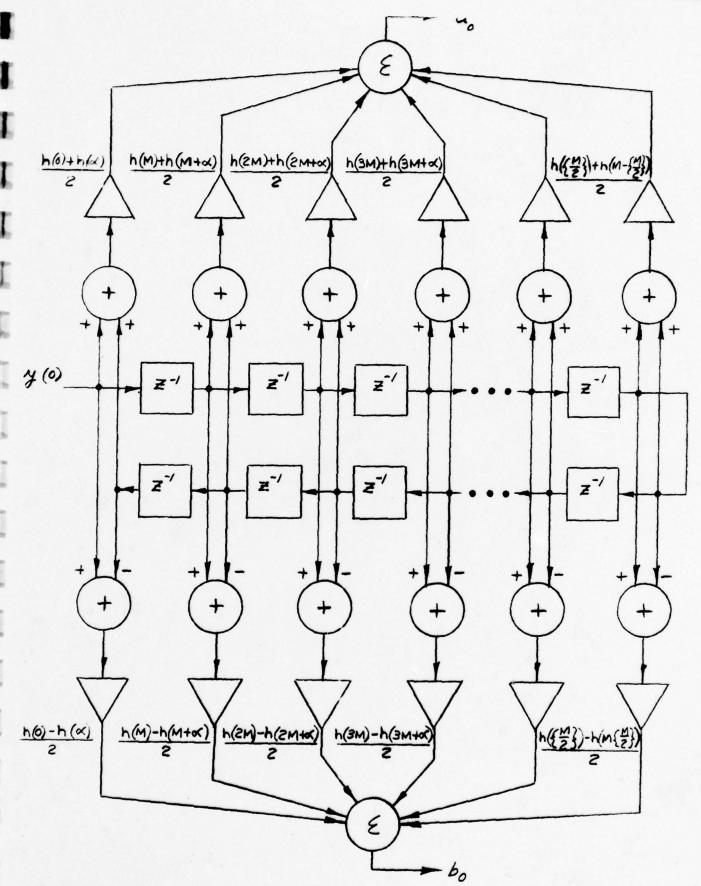


FIGURE 2-7 FILTER STRUCTURE FOR THE NOVEL INTERPOLATION SCHEME 2-26

SUBBAND #	# OF MULTIPLIES PER FRAME IN 9.6 KB/S SYSTEM	# OF MULTIPLIES PER FRAME IN 16.0 KB/S SYSTEM
1	900	330
2	1800	540
3	2020	900
4	3600	1800
5		1800
TOTAL	8320	5370

1

TABLE 2-6 NUMBER OF MULTIPLIES PER FRAME FOR DIGITAL INTER-POLATION WITH NEW TECHNIQUE

2.4 Alternative Subband Coding Techniques

From previous sections, it has been shown that subband coder is a conceptionally simple speech encoding scheme which deals mainly with the partitioning of input speech band into different frequency bands. As detailed in Section 2.2, one approach is to make use of finite-impulse response (FIR) filters to perform the bandpass filtering operation. However, to achieve the necessary bandpass characteristics, it is shown that large order filters are generally needed and this increases the processing burden. Moreover, the combined frequency response of the filter bank may not be desirable as a result of the spectral gaps as depicted in Figures 2-3 and 2-4. Hence, further improvements on performance or simplifications on the implementation of subband coders hinge on the utilization of other bandpass filters.

2.4.1 The Recursive Filter Approach

Since low order recursive filters, somtimes referred to as infinite-impulse response (IIR) filters, are known to yield magnitude response comparable to that of long FIR ones, it would seem feasible to use IIR filters in performing the bandpass filtering procedures in the subband coder. Unfortunately, nonuniform group delay due to the nonlinearity of IIR filter's phase response is rather undesirable for this application. Furthermore, the savings on computations (mainly multiplications) realized through the use of a short filter length is minimal because of IIR filter's inefficiency in performing digital interpolations and decimations.

To illustrate the latter statement, the use of an IIR filter to downsample input samples is considered. If the Z-transform of the IIR filter is:

$$H(z) = \frac{\sum_{i=0}^{N-1} \alpha_i \bar{z}^i}{\sum_{j=0}^{N-1} b_j \bar{z}^j}$$
 (2-28)

where N' is defined as the order of the filter (N' < N), the relationship between the input and the filtered output sample y(n) as depicted in Figure 2-2(a) is:

$$A(u) = -\sum_{n=1}^{2-1} p^{2} A(u-3) + \sum_{i=0}^{2-1} a^{i} x(u-i)$$
(5-53)

Then the downsampled version of y(n) is given by:

$$A'(u) = A(Wu) = -\sum_{i=1}^{j-1} p_i A(Wu-j) + \sum_{i=0}^{j-1} \sigma^i x(Wu-i)$$
 (5-30)

where M is the decimation ratio.

It is clear from Eq. (2-30) that in order to obtain $y_1(n)$, 2N'-1 multiplications have to be performed for every y(n). So, in contrast to the use of FIR filters, the amount of multiplications required in this case does not decrease with M. The use of IIR filters in subband coding is only advantageous over FIR ones if:

or
$$N' \geqslant \frac{1}{2} \left(\frac{N}{2m} + 1 \right) \tag{2-31}$$

As the value of M increases, Eq. (2-31) is less likely to be true and this is one of the reasons that IIR filters may not be applicable for subband coding of speech signals.

^{*}Note: In a recent paper, the design of a special class of IIR filters is given which can perform efficient digital decimation [16]. However, the nonlinear phase characteristic of IIR filters is still undesirable for subband coding.

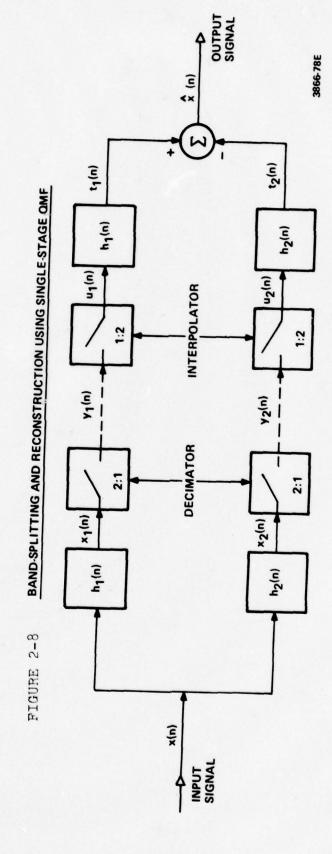
2.4.2 The Quadrature Mirror Filter Approach

A better approach to subband coding is to make use of quadrature mirror filters (QMF) which band-splits/reconstructs the input waveform via decimation/interpolation methods [7] It will be shown later than the use of QMF design equations will achieve perfect splitting/reconstruction without large-order filters.

For explanatory purposes, consider the ideal splitting/ reconstruction process described in Figure 2-8. For this system, the following definitions apply:

- a. x(n) is a Nyquist band-limited signal with z-transform X(z).
- b. h_1 is the impulse response of the low-pass filter and the z-transform of which is $H_1(z)$.
- c. $h_2(n)$ is the impulse response of the high-pass filter the z-transform of which is $H_2(z)$.
- d. $y_1(n)$ is a baseband equivalent low-pass signal with z-transform $Y_1(z)$.
- e. $y_2(n)$ is a baseband equivalent high-pass signal with z-transform $Y_2(z)$.

The signal x(n), is processed by filters $h_1(n)$ and $h_2(n)$ yielding the low-pass and high-pass equivalents, $x_1(n)$ and $x_2(n)$, of the input signal. As their spectra occupy half the Nyquist bandwidth of the original signal, the sampling rate in each band can be halved by decimating (ignoring) every second sample. For reconstruction, the signals $y_1(n)$ and $y_2(n)$ are interpolated, by inserting one zero-valued sample every other time, and then filtered respectivelyby $h_1(n)$ and $h_2(n)$ before being added, to give the signal $\hat{x}(n)$. The dashed lines, shown in Figure 2-8, represent the data



passed to the communication channel(s) by the speech processing system.

In order to minimize $(\hat{\mathbf{x}}(n) - \mathbf{x}(n))$, certain restrictions on the filters, $h_1(n)$ and $h_2(n)$, must be met. We will derive these restrictions by contructing the transfer function of the QMF structure.

Using z-transform notation and referring to Figure 2-8, we may write the intermediary filtered output as

$$X_{1}(Z) = H_{1}(Z)X(Z)$$
 (2-32)

and

$$X_2(z) = H_2(z)X(z)$$
 (2-33)

The transforms of the decimated signals, $y_1(n)$ and $y_2(n)$, and of the interpolated signals, $u_1(n)$ and $u_2(n)$, are given by:

$$Y_{i(2)} = \pm (X_{i}(\frac{2}{2}) + X_{i}(-\frac{2}{2})), \hat{Z} = Z^{1/2}$$
 (2-34)

$$Y_2(2) = \frac{1}{2} (X_2(2) + X_2(-2))$$
 (2-35)

$$U_1(z) = Y_1(z^2)$$
 (2-36)

$$U_2(z) = Y_2(z^2)$$
 (2-37)

After the final filtering operating, the transforms of the reconstructed waveform components, $t_1(n)$ and $t_2(n)$, are given by

$$T_{1}(z) = H_{1}(z) U_{1}(z)$$
 (2-38)

$$T_2(z) = H_2(z) U_2(z)$$
 (2-39)

Using the relations expressed in (2-34) through (2-39), the z-transforms can be rewritten as

$$T_{i}(z) = \frac{1}{2} (H_{i}(z)X(z) + H_{i}(-z)X(-z)) H_{i}(z)$$
 (2-40)

$$T_2(z) = -\frac{1}{2} (H_2(z)X(z) + H_2(-z)X(-z)) H_2(z)$$
 (2-41)

The z-transform of the reconstructed waveform, $\hat{x}(n)$ is obtained by adding (2-40) and (2-41)

$$\chi(z) = \frac{1}{2} (H_1^2(z) - H_2^2(z)) \chi(z) + \frac{1}{2} (H_1(-z) H_1(z) - H_2(-z) H_2(z)) \chi(z^{-42})$$

If we assume that

I

$$H_2(2) = H_1(-2)$$
 (2-43)

then the reconstructed waveform transform becomes

$$\chi(z) = \frac{1}{2} (H_1^2(z) - H_1^2(-z)) \chi(z)$$
 (2-44)

Evaluating z on the unit circle gives the Fourier transform of $\hat{X}(z)$

$$\chi(e^{j\omega T}) = \frac{1}{2} \left(H_1^2(e^{j\omega T}) - H_1^2(e^{j(\omega + \frac{\omega s}{2})T}) \times (e^{j\omega T}) \right)$$
 (2-45)

For the case when $h_1(n)$ is an even, symmetrical FIR filter of order N, then it can be shown that (2-45) reduces to

$$\hat{X}(e^{j\omega T}) = \frac{1}{2}e^{-J(N-1)\omega T}X(e^{j\omega T}) \tag{2-46}$$

where H_1^2 (e^{jwt}) exhibits an odd symmetric property about w s/4 and the half-power point $H_1^2(^w$ s/4) = 0.5.

The inverse transform yields a perfectly reconstructed signal (no frequency distortion) with a gain factor of 1/2 and delay of N-1 samples as shown by

$$\hat{X}(n) = \frac{1}{2} \chi(N-N+1)$$
 (2-47)

Therefore, we have shown that to guarantee perfect reconstruction of the original spectrum, the following filter constraints must be satisfied

$$h_1(n)$$
: symmetrical, even order FIR (2-48)
 $H_2(2)=H_1(-2)$ or $h_2(n)=(-1)^n h_1(n)$; $n=0,1, N-1$ (2-49)
 $H_1^2(2)+H_2^2(2)=1$ (2-50)

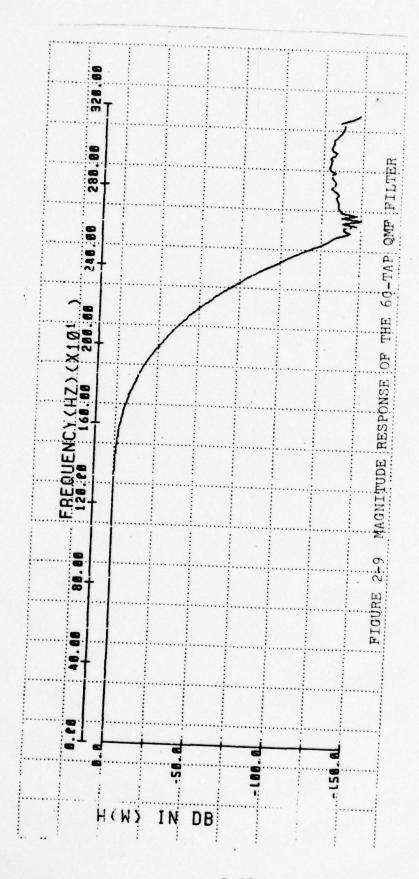
2.4.2.1 Subband Coding via QMF Filters

1

1

Employing a procedure similar to the Hermann design algorithm for maximally flat FIR filters, a 60-tap filter which satisfies the QMF constraints as stated in Eqs. (2-48) to (2-50) is obtained [8,9]. Its impulse response $h_1(n)$ is tabulated in Appendix C and the corresponding magnitude response as depicted in Figure 2-9 shows that the filter has a flat passband extending from 0 - $f_s/4$ Hz. It is also characterized by a fast roll-off with the 3-db point located at $f_s/4$. From $h_1(n)$, its quadrature mirror counterpart $h_2(n)$ is generated using Eq. (2-49).

Starting with these two filters $h_1(n)$ and $h_2(n)$, a new form of subband coder is realized. As a matter of fact, a 3-stage tree structure as shown in Figure 2-10 is exploited to split the input speech band into 8 subbands [10]. For an input signal of 3200 Hz bandwidth, subbands of 400 Hz are resulted. At the first stage of the transmitter, the QMF filters split the input into two bands; that is, 0-1600 Hz and 1600-3200 Hz. Then a downsampling procedure is utilized to reduce the number of samples by a half. At the second stage, the identical bandsplitting process is applied to each subband. Consequently, 2 more subbands are generated each of which has a 800 Hz bandwidth. At the end of the second stage, a total of 4 subbands is obtained. The method is repeated one more time and eight subbands spanning frequency range from 0 to 3200 Hz



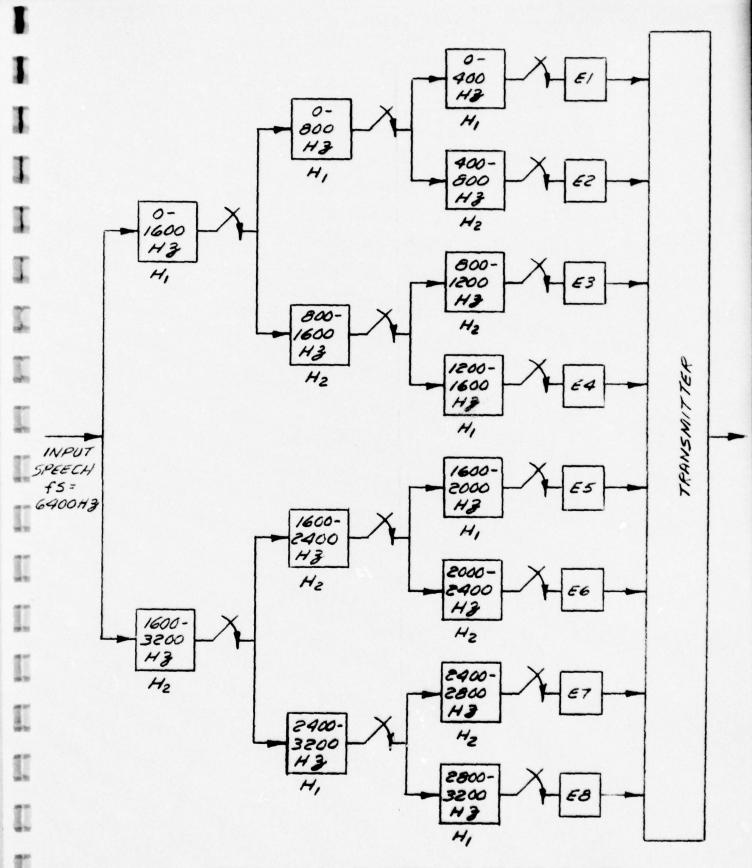


FIGURE 2-10(a) TRANSMITTER OF QMF SUBBAND CODER

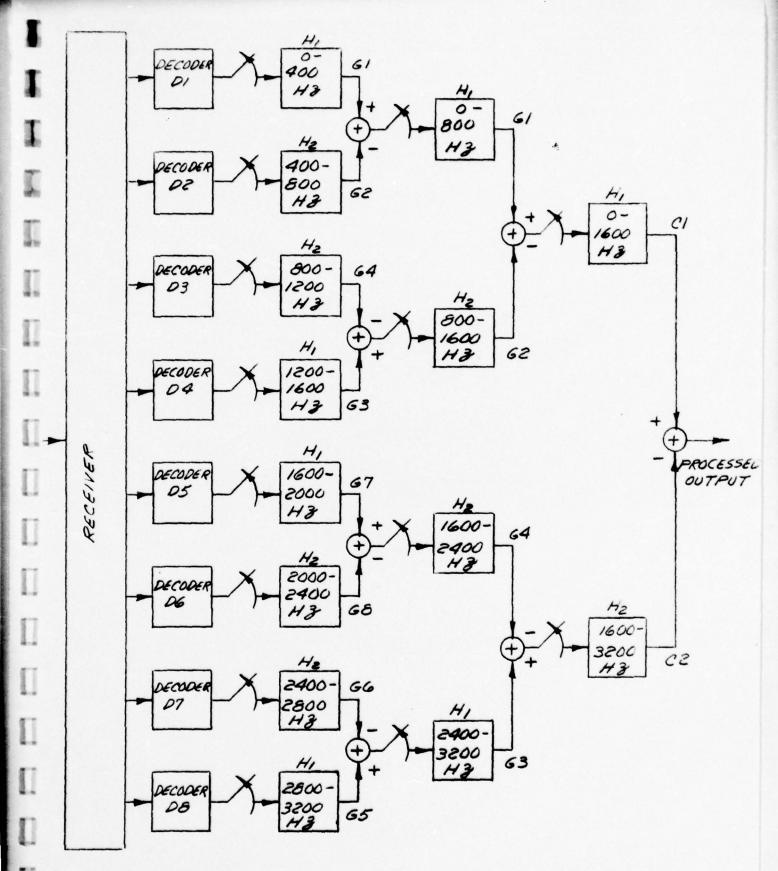


FIGURE 2-10(b) RECEIVER OF QMF SUBBAND CODER

1

are created. After performing the bandsplitting process, the subband signals are individually quantized for transmission. At the receiver, the reverse operation which includes up-sampling and bandpass filtering is performed. They are later recombined to form an estimate of the input signal. So, depending on the number of bits utilized in the quantization of the subbands, both the 9.6 and 16.0 Kb/s subband coders can be realized.

2.4.2.2 Adaptive Bit Allocations

One of the advantages of subband coding algorithms is the possibility of using the spectral densities of the suband signals and applying nonuniform quantization to each one. The conventional approach is to use a fixed-bit allocation rule where a pre-determined number of bits is assigned to the coding of each band. In the QMF system, a larger proportion of the available bits will be allocated to the quantization of the low bands in order to capture all pitch and formant information, whereas a smaller percentage of the bits will be utilized for the high bands. However, since the ratio of low-band and high-band energies fluctuates from frame to frame, fixed-bit allocation may not necessarily be the best strategy. Instead, an adaptive bit allocation scheme that dynamically alters the bit assignments depending on the signal energies of the eight bands seems more applicable [11].

For explanation purposes, let us assume that the average bit rate to quantize all subbands is \overline{R} bits. In other words, if R is the actual number of bits allocated to the ith subband, \overline{R} is given by:

$$\overline{R} = \frac{1}{8} \sum_{i=1}^{8} R_i$$
 (2-51)

The number of bits needed to quantize the ith subband is given by [12].

$$R_{i} = 8 + \frac{1}{2} \log_{2} \frac{\sigma_{x_{i}}^{2}}{\sigma_{x_{i}}^{2}} ; (=1, 2, ... 8)$$
 (2-52)

where $\sigma_{\mathbf{X}_{\mathbf{i}}}^{2}$, $\sigma_{\mathbf{q}_{\mathbf{i}}}^{2}$ denote the power of the ith subband, and the corresponding quantization noise power, respectively, and δ is a correction term which depends on the performance of practical quantizers. If the dependence of R_i on δ is neglected, Equation (2-52) can be rewritten as:

$$\delta_{g_i}^2 = \delta_{\chi_i}^2 \frac{-2R_i}{2}$$
 $(2-53)$

Defining the total quantization noise power E as

$$E = \sum_{i=1}^{8} 6g_{i}^{2}$$
 (2-54)

adaptive bit allocation calls for the selection of $R_{\bf i}$ for each subband such that E is minimized provided the constraint as given in Equation (2-51) is satisfied. This minimization procedure can be best performed with the help of Lagrange multipliers where a combined performance index I, defined as:

$$I = E + \lambda G \tag{2-55}$$

with λ given as the Lagrange multiplier and G the constraint function, is minimized. G is defined as:

$$G = R - \frac{1}{8} \sum_{i=1}^{8} R_i$$
 (2-56)

Differentiating I with respect to R_i and λ , and setting the resulting equations to zero, the following is obtained.

$$\int_{x_{i}}^{2} \frac{-2R_{i}}{2} + \lambda = 0 \qquad ; i = 1, 2, \dots 8$$

$$\overline{R} = \frac{1}{8} \sum_{i=1}^{8} R_{i} \qquad (2-57)$$

Combining Eq. (2-57) for i=1, 2, ... 8,

$$G_{x_1}^2 G_{x_2}^2 \cdots G_{x_8}^2 = \chi^8$$
 (2-58)

Taking logarithm on both sides, substituting Equation (2-57) and eliminating λ , Equation (2-58) becomes

$$R_{i} = \overline{R} + \frac{1}{2} \log_{2} \frac{\sigma_{x_{i}}^{2}}{(\sigma_{x_{i}}^{2} \cdots \sigma_{x_{g}}^{2})^{1/9}} \qquad i=1,2,\cdots 9 \qquad (2-59)$$

Hence, bits to encode each subband can be adaptively allocated according to the corresponding signal power within each band. Furthermore, zero bits are assigned whenever $R_{\rm i}$ as obtained from Eq. (2-59) are negative. To prevent the allocation of all the bits in one subband, a maximum value is imposed on each $R_{\rm i}$. Moreover, the frame powers for the eight subbands have to be transmitted so that the receiver can decode the bits via an identical scheme.

2.4.2.3 Discussion of Results

In order to evaluate the performance of subband coders using QMF filters, simulations of the system are programmed in FORTRAN. Specifications of the 9.6 and 16.0 Kb/s systems are summarized in Table 2-7. In this simulation, a 3-stage QMF filter structure as shown in Figure 2-10 is employed in the bandsplitting and reconstruction. With a filter length of 60 taps, the delay for the entire system is 70*(60-1) or 413 samples.

To examine the effect of the filters, the system is implemented without quantization and Figure 2-11 depicts the overall frequency response of the filter structure. In contrast to the integer-band sampling technique, the QMF filters span the entire speech band with no significant gaps in the spectrum and this results in the "smoother" quality of the processed speech.

To further improve the quality, the adaptive bit allocation algorithm as discussed in Section 2.4.2.2 is also incorporated. In order to prevent the allocation of too many bits on a single subband, a maximum number of 5 bits is allowed. Moreover, for bands with zeroth bit assignment, low level random noise is inserted to eliminate the "low-pass" effect [13]. Though the resulting speech is slightly noisier, the added noise seems to fill the spectral gaps created by quantization of some subbands with no bits and the overall quality of the processed speech is improved.

Figures 2-12 and 2-13 show frame-to-frame signal-to-noise plots for the 9.6 and 16.0 Kbps QMF subband coder. The result indicates that the QMF systems yield relatively high signal-to-noise ratios. Also, the coders seem to perform the best when the input power is highest. This is not surprising since after the bandpass filtering, the subband with the largest average amplitude is captured with the most bits using the adaptive bit allocation

Sampling Rate = 6.4 KHz

Frame Length = 144 samples

No. of Frames/Sec. = 44.4444

Frame Time = 22.5 msec

For the 16.0 Kb/s system: total no. of bits per frame to quantize

8 subbands = 324; Overhead bits per frame = 36

For the 9.6~Kb/s system: total no. of bits per frame to quantize 8

subbands = 180; Overhead bits per frame = 36

SUBBAND #	FREQUENCY RANGE IN HZ	DOWNSAMPLING (INTERPOLATION) RATIO FOR ALL 3 STAGES	QUANTIZER BIT ALLOCATIONS
1	0- 400	8	adaptive
2	400- 800	8	adaptive
3	800-1200	8	adaptive
4	1200-1600	8	adaptive
5	1600-2000	8	adaptive
6	2000-2400	8	adaptive
7	2400-2800	8	adaptive
8	2800-3200	8*	adaptive

TABLE 2-7 SPECIFICATIONS OF 9.6 AND 16.0 KB/S QMF SUBBAND CODERS

63																										
320.036									.i,		!		·	į				·								
60	Γ Ι			••••••								•						· · · ·	·····							
280.00																										
286	- <											·	·						·							
	1																									
88	1												 !						 !							
240.00	1																						****			 * * *
2)		.i																						*****	
60	-/											·,														
60	- 7			·!···														• • • •		DER						
200.00)										• • • • •			• • • • • • • • • • • • • • • • • • • •					2						
1																	• • • • • • • • • • • • • • • • • • • •			RND	• • • • • • • • • • • • • • • • • • • •					
. 68	/																			SUBBAND CODER						
199	{			· · · · ·											:					F.S		- :				
120.00 160.00	···/																			DMF			:			
90		.i									••••				••••	• • • • • •	•••••	• • • • •		TRP		:		•••••		
20.	2)																••••	••••	6.0			:			
			į																							
	···/																			RESPONSE						
80.00)													••••					;	RES		• • • •				
8							••••			••••	••••	••••		•••••	••••	••••		• • • • • • • • • • • • • • • • • • • •	•••••		•••••	·				
	/.																			SPECTRAL	• • • • • • • • • • • • • • • • • • • •					
48.88																				SPE						
4.6	3																									
	1				••••		••••		••••	• •••	••••	•••••	•••••				••••									
										•••••		••••								压	•••••		•	·		
9.00	-					_		_								_				FIGURE 2-11.		:				
	8							2.0				3.0				4.0				E						
					••••											4										
		ı	10	W.).		N.	D	R:			2	-4	3													
				× .2.		. IX.		D			• • • • •				••••••											 -

I

I

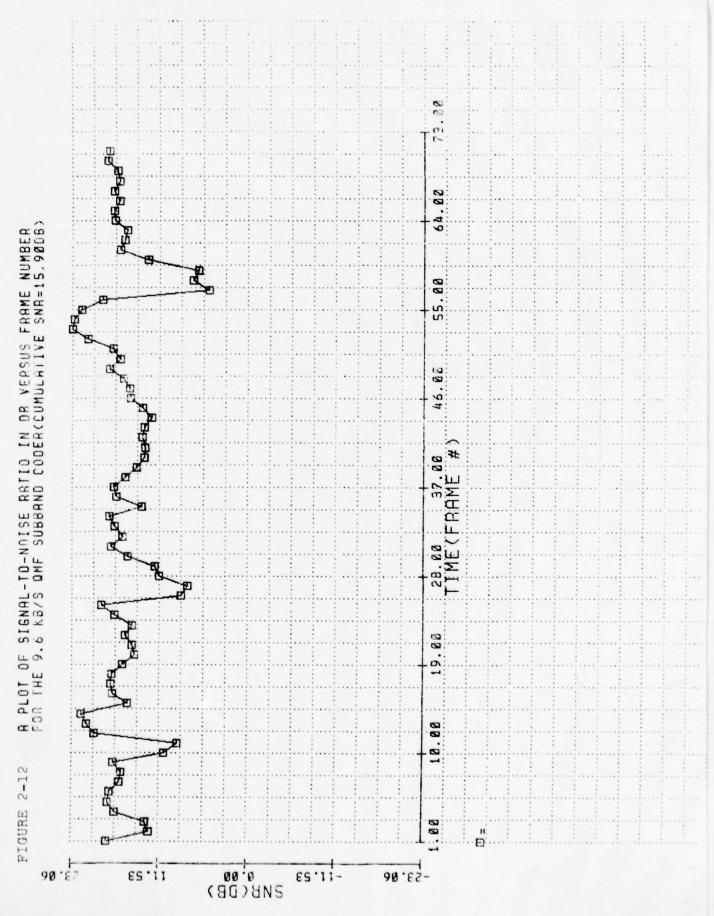
I

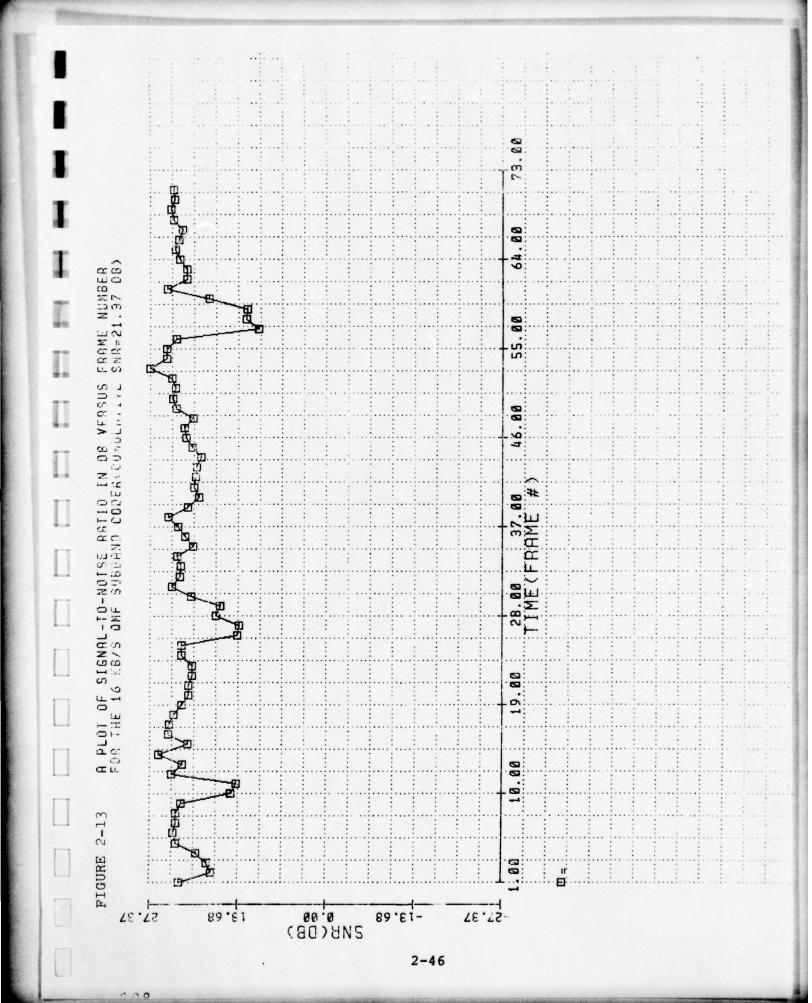
rule. Informal listening tests conducted on processed sentences also show that the speech quality of QMF subband coder is improved over that of the integer-band sampling technique. At 9.6 Kb/s, the system tends to produce slightly reverberent speech and however at 16 Kb/s, high quality speech is yielded.

1

1

1





SECTION III

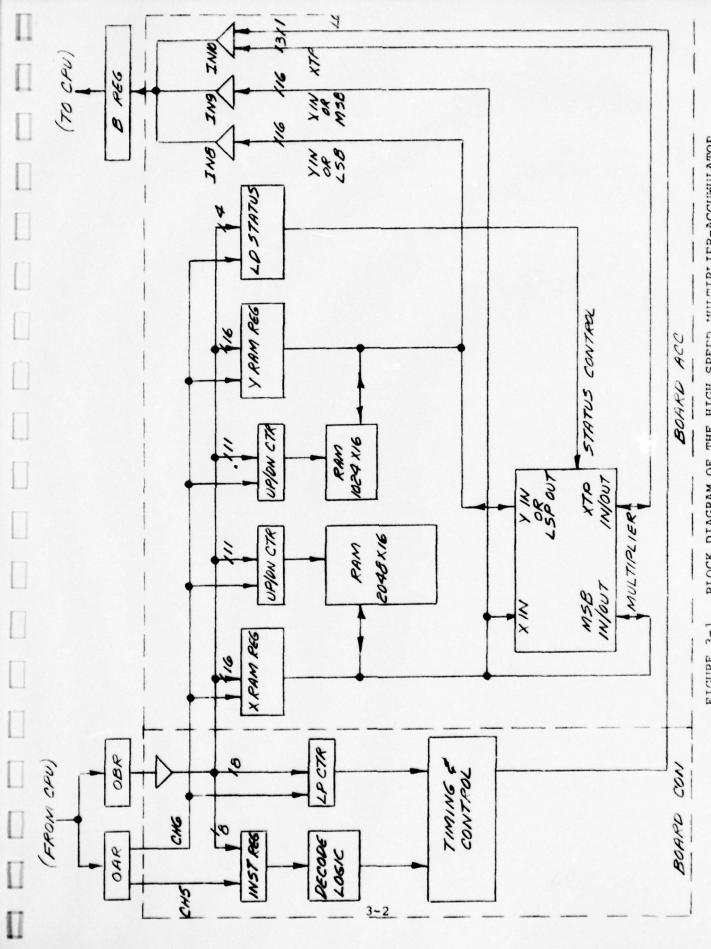
The Multiplier-Accumulator Hardware

3.1 General Description

In this contract, GTE Sylvania developed a state-of-the-art multiplier-accumulator (MULACC) which greatly enhances the capability of the Sylvania Programmable Signal Processor (PSP) in various signal processing applications. In addition to linear convolutions, the hardware performs computations of auto-/crosscorrelation of two arrays of numbers most effectively. The nucleus of the design is a high speed 64-pin multiplier-accumulator chip (TRW TDC 1010J) which multiplies two 16-bit numbers and accumulates a 35-bit product in 115 nsec. Moreover, to fully exploit its capability, two buffers of fast RAM memories (MOSTEK MK4118P) are included which feed data directly into the chip. Since the circuitry communicates with the PSP CPU through input/output buses, these memory buffers drastically reduce the passing of data between the PSP and MULACC. Furthermore, since MULACC is treated as a peripheral, no hardware changes are required on the PSP CPU and all existing programs are still operable on the modified machine. After starting MULACC, the PSP CPU is also free to perform other tasks and this represents a more efficient utilization of available processing time. As an indication of its speed, the MULACC is capable of accessing the data from the two buffers, multiplying two 16-bit numbers, and forming a 35-bit product accumulation in 208 nsec (or 2 PSP cycles).

The MULACC hardware as shown in Figure 3-1 consists of two PC cards. The first card (board CON) , located at slot 7 of the PSP nest, is responsible for interpreting outputs from the PSP CPU, and decoding them into MULACC instructions. In particular, outputs from channel 5 of the PSP are converted into MULACC instructions whereas outputs from channel 6 are treated as data. Then the correct calling sequence for programming MULACC becomes

- 1) OUT 5 INSTRUCTION
- 2) OUT 6 DATA



BLOCK DIAGRAM OF THE HIGH SPEED MULTIPLIER-ACCUMULATOR FIGURE 3-1

After the first line of code, the instruction register of MULACC is loaded and the corresponding timing and control information are read from a programmable logic array (PLA). This is later used to setup the sequence of operations required by the instruction. From the second line of code, the data become operands of the corresponding memory registers and loopcounters.

The second PC card (board ACC) located at slot 5 of the PSP nest, contains the two buffer memories as denoted by X and Y, and the multiplier-accumulator chip. Memory address registers which are also present on board ACC can be programmed to point to any locations within the buffers. An up/down counter is utilized to increment/decrement the address registers automatically after each memory access. In the present design, 2K 16-bit data points can be pre-stored in X-buffer whereas 1K can be loaded into Y-buffer. After MULACC is started with setting of the loop counter, 32-bit product is first formed which is then added to the content of the TRW chip's output register. Upon the termination of the operation, a LOAD bit is set to a 1 and the 35-bit product is then transferred to the PSP input channels in three segments; namely, extended, most significant, and least significant products.

3.2 Programming of MULACC

As discussed in Section 3.1, procedures for programming MULACC include the outputting of an instruction code from channel 5 of the PSP, followed by an output of data from channel 6. From the first output, the instruction register of MULACC is loaded and the second output supplies the operand data. MULACC instructions, which include the loading of X and/or Y buffer addresses and memories, the selection of multiplier functions, and loading of multiplier loop counter are listed in Table 3-1.

As for multiplier functions, the hardware permits the choice of 12 functions; namely, unsigned magnitude/2's complement arithmetic, multiplication with/without rounding, multiplication with/without accumulation, multiplication with/without subtraction, increment/decrement of X-buffer pointers, and increment/decrement of Y-buffer pointers. Bit settings of the corresponding functions

TABLE 3-1 MULACC INSTRUCTIONS

I

I

I

П

INSTRUCTIONS	HEX VALUES	COMMENTS
Idle (IDLE)	0	An output of value 0 to channel 5 will set the MULACC to an idle state
Load X-Buffer Address (XADR)	1	Outputs of value 1 to channel 5, followed by the number XXXX to channel 6 will point to address XXXX of X-Buffer $(0 \le XXXX \le 2047)$.
Load Y-Buffer Address (YADR)	2	Outputs of value 2 to channel 5 followed by the number YYYY to channel 6 will point to address YYYY of Y-Buffer (0 \(\(\Lambde{L}\)\) YYYY \(\Lambde{L}\) 1023).
Load Identical X-Buffer and Y-Buffer addresses (ADR)	3	Outputs of value 3 to channel 5, followed by the number XXXX to channel 6 will set both X and Y-Buffer address pointers to XXXX.
Load X-Buffer Memory (LDX)	4	Outputs of value 4 to channel 5, followed by the number DDDD to channel 6 will load data DDDD into the pointing X-Buffer address (see Note 1 in Table 3-4).
Load Y-Buffer Memory (LDY)	5	Outputs of value 5 to channel 5, followed by the number DDDD to channel 6 will load data DDDD into the pointing Y-Buffer address (see Note 1 in Table 3-4).
Load Identical Values into X and Y-Buffer Memories (LXAY)	6	Outputs of value 6 to channel 5, followed by the value DDDD to channel 6 will load data DDDD into the pointing X and Y-Buffer addresses (see Note 1 in Table 3-4).
Select Functions (TASK)	7	Outputs of value 7 to channel 5 followed by the value DDDD to channel 6 set up the MULACC to perform task DDDD. (Refer to table 3-2 for specific task definitions.)
Read Multiplier (READ)	8	An Output of value 8 to channel 5 followed by a waiting period of 4 cycles will enable the products presently residing at the MULACC to be read (see Note 2 and refer to Table 3-3 for specific reads).
Load Loop Counter & Start Multiplier (LOOP)	9	Ouputs of value 9 to channel 5 followed by the number (255-nnn) to channel 6 will set up the MULACC to multiply nnn times. The maximum number allowed is 255. Immediately after the setting of the loop counter, multiplication begins.
Load different addresses of X and Y- Buffers (XYADR)	A	This is a short cut to load different X and Y-Buffer addresses. Outputs of value A to channel 5 followed by a value of XXXX to channel 6 and a value of YYYY to channel 6 will set the X and Y address pointers to XXXX and YYYY, respectively.

are summarized in Table 3-2. To illustrate this, the selection of multiplication with accumulation function is considered. First, a value 7 is outputted from PSP channel 5 to MULACC which signifies the choice of functions. Then an output of (33)₈ from channel 6 sets up MULACC to perform 2's complement arithmetic, multiply (with no rounding) with accumulation, and increment both X and Y buffer pointers after each operation. Hence, by resetting the buffer pointers, the multiplier can be started to perform multiplications with accumulation of two arrays of numbers.

When the multiplier is finished, the load (RDY) bit of MULACC will be set to 1 and the results can be transferred. Since the PSP is a 16-bit machine, the 35-bit product is shipped via three input channels; namely, the extended product (XTP) through channel 10, the most significant product (MSP) through channel 9, and the least significant product (LSP) through channel 8. In addition, the RDY bit is multiplexed with the actual XTP during the transfer. So, after reading the XTP, the PSP has to perform a masking followed by a shift right once operation in order to obtain the correct XTP.

Besides the products, input channels 8 and 9 are also utilized to read the X and Y buffer memories. A tri-state device gating on the multiplier RDY bit is used to switch the outputs from the multiplier to that of the memories. In particular, when RDY = 0, input channels 8, 9 are connected to that of Y, X buffers, respectively. On the other hand, if RDY = 1, input channels 8, 9, 10 are hooked up to LSP, MSP, XTP. PSP instructions required to read products and memories are shown in Table 3-3. Also, special considerations on loading and reading of MULACC buffers, together with multiplier functions are discussed in Table 3-4.

To further illustrate the utility of MULACC, a PSP demonstration program that computes the following operation is detailed in Figure 3-2:

$$y(0) = \sum_{k=0}^{\Sigma} h(k) x(0-k)$$
 (3-1)

TABLE 3-2 MULTIPLIER FUNCTIONS

**	B1T 5	BIT 4	BIT 3	BIT 2	BIT 1	BIT 0
BIT SETTING = 0	DY	DX	NO RND	NO SUB	NO ACC	USM
BIT SETTING = 1	IY	IX	RND	SUB	ACC	тс

Symbol Definitions:

I

-

USM: Unsigned magnitude arithmetic (16-bit with no sign bit)

TC: 2's complement arithmetic (15-bit with 1 sign bit)

ACC: product accumulation (ACC = Product + ACC)

SUB: product subtraction (If bit 2=1 & bit 1=1, ACC = PRODUCT - ACC)

IX : increment X-buffer pointer

DX : decrement X-buffer pointer

IY: increment Y-buffer pointer

DY: decrement Y-buffer pointer

RND: rounding (see Note 3 on Table 3-4)

TABLE 3-3 INSTRUCTIONS TO READ BUFFER MEMORIES AND MULTIPLIER PRODUCTS

1	INSTRUCTIONS	PSP MNEMONICS	COMMENTS				
	To read contents of X-Buf∵er (XREAD)	INPA 9.	After setting up the X-Buffer address using XADR, its content can be read after a waiting period of 4 cycles				
	To read contents of Y-Buffer (YREAD)	INPA 8.	After setting up the Y-Buffer address using YADR, its content can be read after a waiting period of 4 cycles				
	To read the content of extended product (XTPR)	INPA 10.	Following either a load loop counter (LOOP) or read multiplier (READ) instruction, the extended product (ATP) can be accessed. Only the lower four bits are of interest and the upper 12 bits should be masked out. Its format is as follows: 15				
			where RDY=0: multiplication has not been completed RDY=1: multiplication has been completed The XTP is meaningful only if RDY=1				
	To read the content of the most significant product (MSPR)	INPA 9.	Following either a load loop counter (LOOP) or a read multiplier (READ) instruction, the most significant product (MSP) can be read. However the MSP value is valid only after the multiplication has been completed (i.e., RDY=1)				
	To read the content of the least significant product (LSPR)	INPA 8.	Following either a load loop counter (LOOP) or a read multiplier (READ) instruction, the least significant product (LSP) can be read. The LSP value is valid only after the multiplication has been completed (i.e., RDY=1)				

TABLE 3-4 NOTES ON PROGRAMMING THE MULACC

Loading of X and/or Y-Buffer Memories

I

Since the loading of buffer memories takes more than two cycles, a 4-cycle wait period is needed to assure the success of writing consecutive memory locations.

2. Reading of Buffer Memories and Multiplier Products

The MULACC functions include the readings of buffer memories and the three multiplier products. In executing instructions that do not involve the multiplier, the product outputs are disenabled from the tri-state control and the bus is connected to the buffer memories which allows the reading of their contents. At this time, the multiplier ready bit is reset (RDY = 0). However, by outputting a read multiplier (READ) instruction on channel 5, the tri-state bus is switched to the multiplier outputs. This set the RDY bit to 1 and enables the reading of existing multiplier products.

In performing operations that require the multiplier, the RDY bit, originally set to 0, will change to a 1 immediately upon their completion. At this time, the three products will be ready to be transferred to the PSP using instructions shown in Table 3-2.

3. Multiply with Rounding

The TRW chip has a multiply with or with no rounding option. The multiply with rounding is performed by adding a 1 to bit 15 of the least significant product and the rounded result is obtained by reading the extended and most significant products. This option is generally not recommended for multiplication together with accumulation since it yields erroneous results. To further illustrate this, the multiplication with rounding and accumulation of two arrays of 0's shows a non-zero final value.

Block 1 of the program chooses the multiplier functions whereas Block 2 indicates the loading of the X and Y buffer memories. As shown in the figure, the starting addresses of the buffers are first set and then each MULACC buffer location can be individually loaded from PSP memories. By resetting the buffer pointers (X pointing to h(0), Y pointing to x(0)), the loop counter is initialized to be 200 and multiplication with accumulation is started as shown in Block 3. The multiplier RDY bit is constantly checked and results are transferred to PSP as illustrated in Block 4.

JLACC TO PERFORM -199)		SAME OF CODE AS OUTH 5,0000 SAME OP CODE AS INPA 8. READ THE LEAST SIG. PART OF PRODUC SAME OP CODE AS INPA 9. READ THE MOST SIG. PART OF PRODUCT SAME OP CODE AS INPA 9. READ THE EXTENDED PART OF PRODUCT	MALTIPLY WITH NO ROUNDING PRODUCTION AND THE POINTER POINTER TO INCREMENT Y BUFFER POINTER		'SBLECT MILACE FUNCTION 'SBLECT MITH ACC, INCR. X AND INCR. Y	SET UP TO LOAD BOTH ADDRESSES OF BUFY AND BUFY	SET UP COUNTER TO LOAD 200 COEFS SET UP INSTRUCTION TO LOAD X MENORY PICK UP FILTER COEFS . PRO STORE IN BURX LOOP UNTIL ALL 200 COEFS ARE FINISHED	SET UP COUNTER TO LOAD 399 SAMPLES IN BUFFER Y
TITLE DEMO, PAP THIS PROGRAM DEMONSTRATES THE USE OF MULACC TO PERFORM BANDPASS FILTERING Y(0)=H(0)X(0)+H(1)X(-1)++H(199)X(-199)	REGISTER FILE DEFINITION	. COMPRIND DEFINITIONS SETUP-132400 DO-3140 LSPR-4040 MSPR-4440	MULACE FUNCTION DEFINITIONS XLN=01 HCC=02 IX=20 IY=40	PROG 10	INST SETUP, TASK LDAL XLNIACCIIXIIY INST DO	LOADING OF BUFFERS X AND Y SETUP, ADR LDAL 0	LOAD FILTER COEFFICIENTS INTO X BUFFER LDRL 200,-1.R1 SETUP, LDX LDA H .R1 DO XLOAD,R1	, LOAD INPUT SAMPLES INTO Y BUFFER LDRL 200.+1991,R1
K-1. C					0		(O) S	
V31	000000001	000000E508 0000000E50 0000000E20 0000000E20	000000001 000000000 000000010 000000000	8000000000	9008 B500 9005 9009 7443 9033 900A 9660 9000	900B B500 0002 9007 7643 9000 9000 9660 9000	000E 3441 00C7 000F B500 0003 0010 CG21 01B5 0011 0660 0000 0012 1141 0010	0013 3A41 018E
				พิพิพิ 3-10			<u>1</u> 44444444	

I

I

A PSP PROGRAM TO DEMONSTRATE THE UTILITY OF MULACC FIGURE 3-1

FIGURE 3-1

SET UP TO LOGG Y BUFFER WITH MENORY CONTENT FROM INPUT BUFFER YOOP UNTIL ALL 399 SAMPLES ARE DONE	RESET THE X BUFFER POINTER TO BE AT 8 RESET THE Y BUFFER POINTER TO BE POINTING AT 180 OR INPT(8) PESSET LOOP COUNTER TO PERFORM 288 PLITTIRLY AND ACCUMULATES	PERSON THE EXTENDED PRODUCT COPPING IF NO IS REPOY BIT SET? CONTINUE LOOPING IF NO	'IF READY, SAVE ONLY 4 LONER BITS SHIPT RIGHT ONCE TO GET RID OF READY BIT STORE IN MENORY LOCATION XTP	'IF READY, READ THE MOST SIGNIFICANT PRODUCT STOKE IN MEDRY LOCATION MSP	'IF READY, READ THE LENST SIGNIFICANT PRODUCT STOKE IN MEMORY LOCATION LSP	INSTRUCTION TO LOAD X BUFFER ADDRESS INSTRUCTION TO LOAD Y BUFFER ADDRESS LOAD IDENTION. ADDRESS IN BUFX AND BUFY LOAD DATA INTO BUFY SELECT FUNCTIONS SELECT FUNCTIONS SELECTION TO STORE EXTRADED PROJECT LOCATION TO STORE THE LOST SIG. PROJUCT LOCATION TO STORE THE LOST SIG. PROJUCT LOCATION TO STORE THE LOST SIG. PROJUCT FILTER ADDRESS X(4) X(1) X(173) INPUT BUFFER X(6) X(1) X(173) INPUT BUFFER X(6) X(1) X(173)	
SETUP, LDY, LDY, DO NO. P1. NO. P1. NO. P1. NO. P1. P1. P1. P1. P1. P1. P1. P1. P1. P1	ACCUPAL MITH MUACC SEED! A ABOR LIDAL 8 SEED! YAD!R UDAL 188. SEED!P, CLOOP SEED!P, CLOOP DO SEED!P, 255288.	XTPR 0.WAIT	PAOL 15. SR1 STA XTP	MSPR STA MSP	LSPR STH LSP	DATA OF STARTS HERE. DATA OF STARTS HERE. BLOCK 199. BLOCK 199. BLOCK 200.	
ο,	MULTIP-Y AND INSTITUTE AND INS					28.88 8.888	
PO. PA LINST LINST		.INST		 F8		### ##################################	
7.090s	Õ	LINITS	6	5		6 66666666666666666666666666666666666	
B500 8884 CG21 8084 0650 8880 1141 8015	######################################	8428 8888 2828 8821	7843 989F 409B 9898 FF99 9887	99528 8888 FF-88 8888	9820 9880 FF00 9899	88888888888888888888888888888888888888	
28888 48861	88888888888888888888888888888888888888	8821	888 848	888	88	888888888 8888 810020 866866418	
្តិ ១೯:	8828888888888	ዻ፟ፙጜ፞፞፞	\$3895	883 3-1		ਫ਼ਫ਼ਫ਼ਫ਼ਖ਼ਲ਼ਖ਼ਖ਼ਖ਼ਖ਼ਖ਼ਖ਼ਫ਼ਫ਼ਫ਼ ਫ਼ਫ਼ਫ਼ਫ਼ਫ਼ਫ਼ਫ਼ਫ਼ਫ਼ਫ਼	

SECTION IV

Real-Time Software

4.1 Introduction

The real-time subband coder programs, operating at the data rates of 9.6 and 16.0 Kb/s, perform subband coding of speech signals via the integer-band sampling technique [3]. Exploiting a high speed multiplier-accumulator (MULACC), the 9.6 Kb/s program runs in a full-duplex mode whereas the 16.0 Kb/s program operates in half-duplex on the PSP. A summary of the real-time 9.6 and 16.0 Kb/s subband coder specifications is shown in Tables 2-1 and 2-2. The functions in the real-time program include speech/line side interrupt processing; receiver/transmitter synchronization; decimation/interpolation filtering; and quantization/dequantization of subband waveforms.

Under the speech side interrupt control, speech samples are brought into the PSP via the A/D converter and, concurrently, processed speech is outputted through the D/A. After subband filtering and encoding of the input signal, the binary bit stream is then transferred from one PSP to the other using the line side interrupt.

Within each frame of transmitted data, a synchronization (SYNC) bit is inserted at the same position of the frame. Through an extensive handshaking procedure, the receiver synchronizes with the transmitter by determining the position of the SYNC bit and eventually aligns the received data buffer to that of the transmitted one. In the real-time programs, the sync bit is set alternatively to a 1 or 0 to assure a more reliable synchronization between the two PSP's.

A major portion of the subband coder's processing load lies on the decimation and interpolation filtering in the main line code. At the transmitter, this involves the filtering of digitized speech samples using a bank of 4 or 5 finite-impulse-response (FIR) filters, each of which is 200-tap long, and the downsampling (decimating) of the output. These decimated subband signals are then quantized for transmission. At the receiver, the transmitted values are dequantized, up-sampled (interpolated), and filtered through the same bank of filters. The outputs are later combined to form an estimate of the input signal. The following sections describe in more detail the operation of each program function.

4.2 Speech/Line Side Interrupts

1

The speech side interrupt is responsible for transferring speech data into and out of the PSP's. Its interrupt rate is basically controlled by a programmable real-time counter (OOOF₁₆) and an I-O clock whose frequency is 11.52 MHz. Dividing the frequency of the clock by the setting of the counter yields the desirable sampling rate of the speech signal.

At every occurrence of a speech side interrupt, the program control is transferred to program counter = 0, which contains an instruction to jump to the speech side interrupt servicing routine where a speech sample is inputted to the speech buffer from the A/D converter and then a processed one is outputted to the D/A converter. The program utilizes a double buffering scheme on both the input and output buffers which allows the processing of a frame of data simultaneously with I/O accessing of the other. The speech side interrupt also sets flags and pointers indicating which buffers are being loaded or transmitted. Figure 4-1 describes in detail the operations of the speech side interrupt.

Similar to the speech side interrupt, the transfer of binary data from one PSP to the other is controlled by the line side interrupt whose rate is set by a second real-time counter (000E16). At every occurrence of the interrupt, program control is sent to the line side interrupt servicing routine starting at program counter = 1 where transmission and reception of bit streams are performed. For the line side transmitter, the PSP hardware is set up in such a way that it takes two interrupts to generate 1 transmitter clock cycle (a high clock bit followed by a low one). At the same time, the identical data bit is outputted throughout the entire clock cycle. So, in order to achieve a particular data rate, the line side has to be interrupted at twice the data rate. For example, the line side interrupt rate has to be set at 32 KHz for 16 Kb/s transmission. As for the line side receiver, the routine inputs an 8-bit word on every 16th interrupt. Then each of these bits is unpeeled and a histogram of all receiver bits is compiled counting the number of times a 1 is received in each bit position. The histogram information is later used during the sync search. A flow chart description of the line side interrupt is depicted in Figure 4-2.

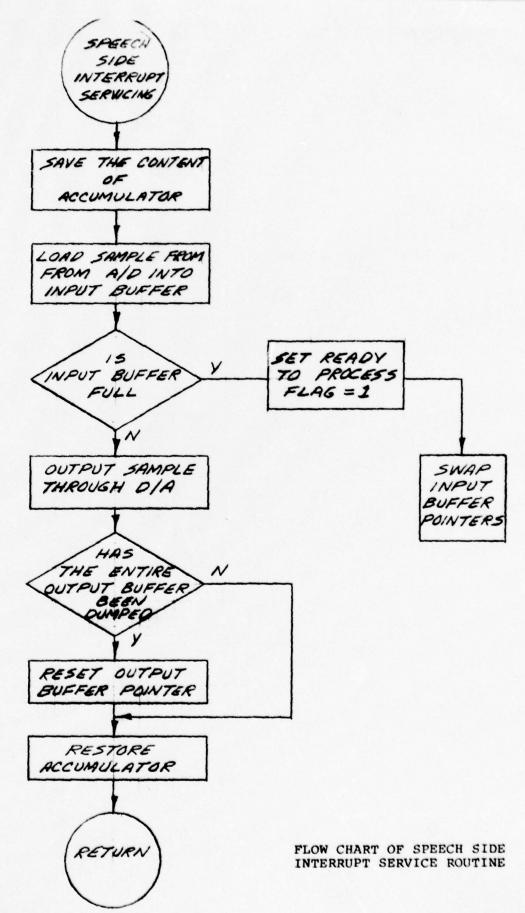
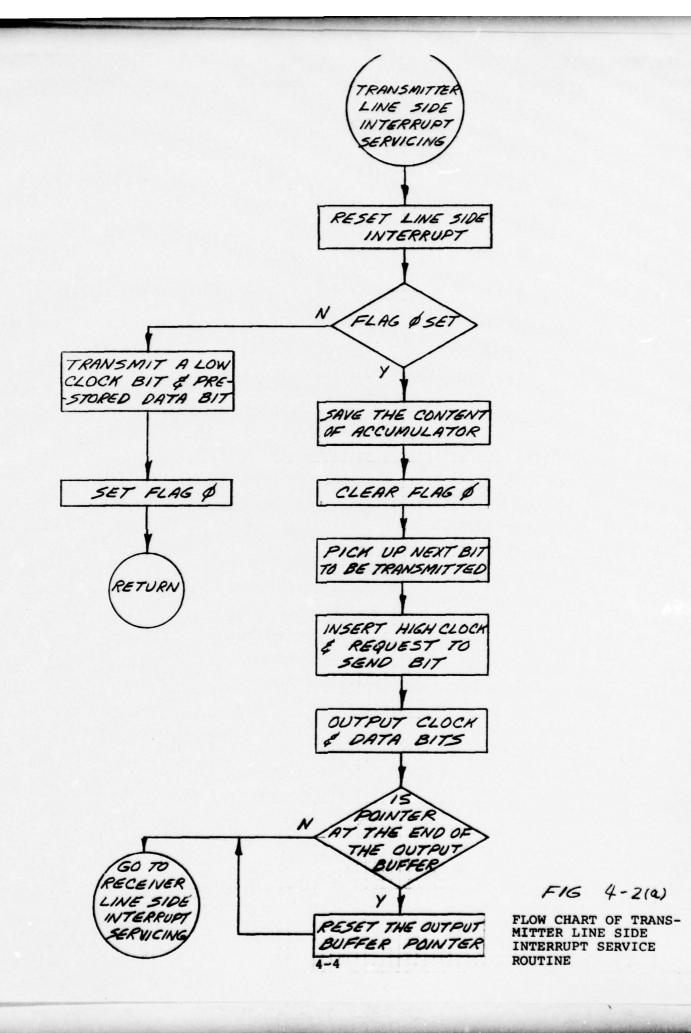
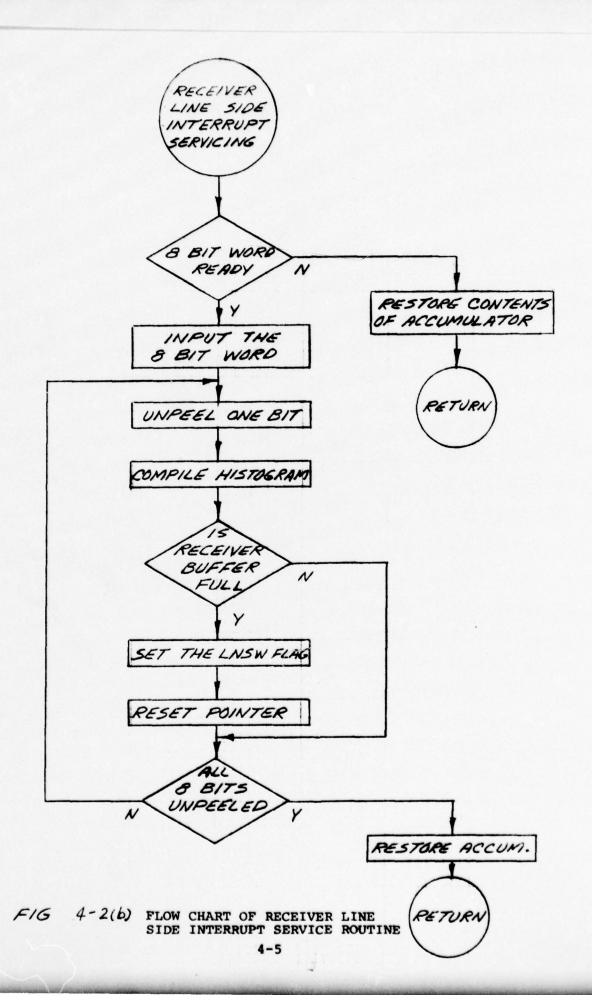


FIG 4-1





4.3 Initialization and Wait Loop

In the operation of the real-time program, the very first function is the initialization routine which sets most of the program variables prior to processing. All flags and storage buffers are cleared together with loading of the line and speech side real-time counters. Band-pass filter coefficients needed to perform decimation and interpolation filtering for all subbands are loaded into the X-buffer of the high speed multiplier-accumulator (MULACC). Figure 4-3 illustrates the storage of these coefficients. Also, quantizer/dequantizer parameters and index registers are loaded with their initial values. Upon exiting from the initialization routine, the speech and line side interrupts are enabled and program control is then transferred to the wait loop.

Figure 4-4 is a flow chart description of the wait loop. Since not all of the available processing time is used in the real-time subband coder programs, the wait loop consumes all the idle time left over. It also correctly sequences the transmitting and receiving operations by examining the transmitter and receiver ready flags and interrogates the front panel to see if reinitialization is desired.

4.4 Transmitter/Receiver Synchronization

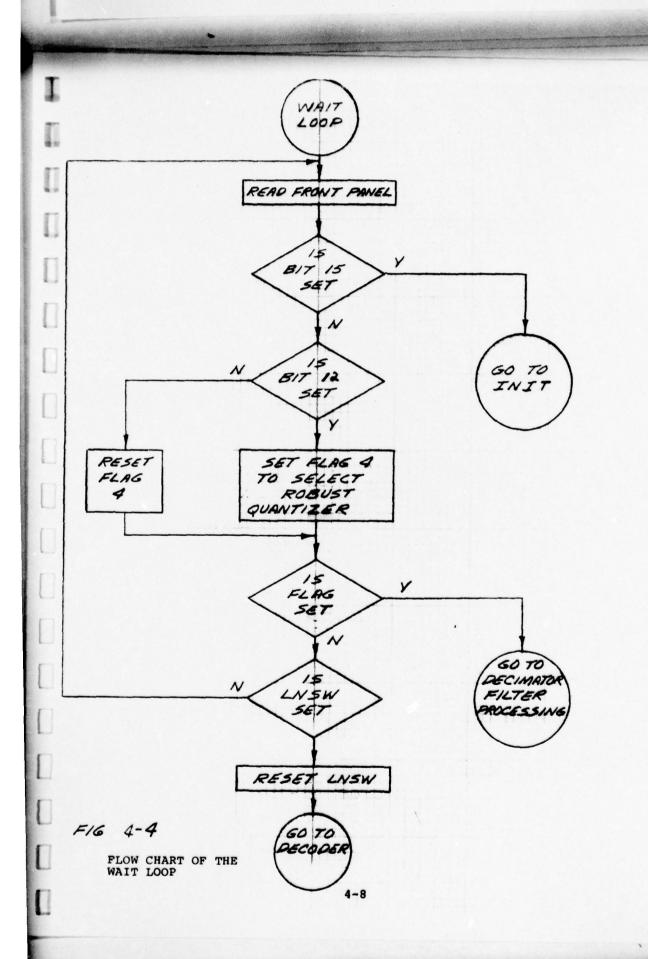
After quantizing the subband signals, the transmitter data buffers in the real-time program are set up to have unused bits. In particular, there are 5 bits left over in the 9.6 Kb/s and 4 in the 16.0 Kb/s systems. One of these available bits is allocated in the programs for synchronization purposes. This bit, generally referred to as the SYNC bit, is set to a 1 or 0 every alternate frame. Utilizing a search procedure for this SYNC bit, the receiver is able to locate the beginning of the received buffer for proper decoding of the transmitted data. The sync search routine is performed on every 80th pass (or 675 msec) through the receiver codes in the 16.0 Kb/s system and on every 40th pass (or 750 msec) in the 9.6 Kb/s system. During the remaining times, the receiver line side compiles a histogram which tallies the times that a 1 has been received in each bit

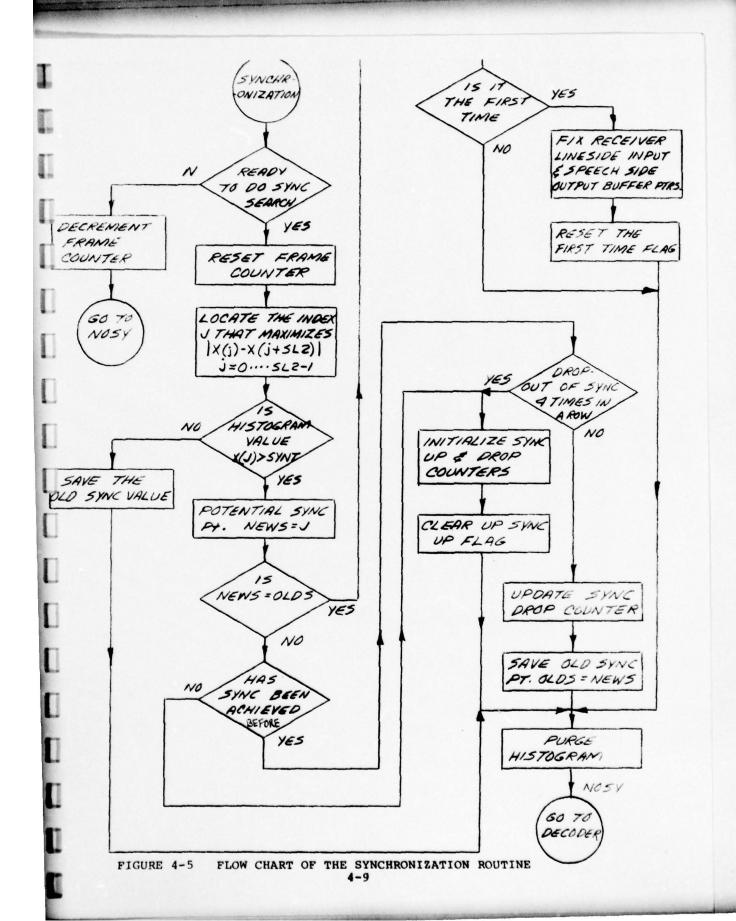
This is a short cut to load different X and Y-Buffer addresses. Outputs of value A to channel 5 followed by a value of XXXX to channel 6 and a value of YYYY to channel 6 will set the X and Y address pointers to XXXX and YYYY, respectively.

3-4

	9.6 Kb/s X-Buffer	Location	16.0 Kb/s X-Buffer	Location
	Filter Coefficients for Band 1	0 - 199	Filter Coefficients for Band 1	0 - 199
	Filter Coefficients for Dand 2	200 - 399	Filter Coefficients for Band 2	200 - 399
	Filter Coefficients for Band 3	400 - 599	Filter Coefficients for Band 3	400 - 599
	Filter Coefficients for Band 4	600 - 799	Filter Coefficients for Pand 4	600 - 799
	Interpolator Coefficients	800 - 1606	Filter Coefficients for Band 5	800 - 999
	-2	_	Interpolator Coefficients	1000 - 2025
			1	
L				

FIGURE 4-3
Storage of Filter Coefficients in MULACC





position within the two data buffers. The sync position is then located by computing the absolute difference between the histogram values of the present bit position and that of the bit situated one frame apart. The bit position that corresponds to the largest difference is defined as the sync point. To assure that the correct sync point has indeed been found, sync search is repeated two more times. If the sync point is identical in all 3 cases, the true one is located. Otherwise, the sync search is resumed until three identical sync points are consecutively found. After achieving synchronization, the sync search is still performed. A sync drop counter is utilized to keep track of the failure of synchronization. As a matter of fact, if the two PSP's are out of sync five times, resynchronization is auto-Figure 4-5 is a flowchart description of matically repeated. the synchronization routine.

4.5 Decimation Filtering

Once the initialization and synchronization procedures have been completed, the PSP's are ready to process the input speech. As described before, the transmitter ready flag (FLAG) is constantly examined in the wait loop to determine when a frame of new speech data has been loaded. When FLAG is set, program control is transferred to the transmitter routine whose major functions include decimation filtering.

Upon entering the transmitter code, a sync pulse is outputted for timing purposes and FLAG is reset. Then the filter memories are updated together with the loading of a new frame of speech data.

The decimation filters decompose the incoming speech signal into four (in the 9.6 Kb/s system) or five (in the 16.0 Kb/s system) subbands. The integer band down-sampling method is used to perform the low-pass translation of each subband. The speech samples stored in the decimation filter buffers are loaded into the Y-array of MULACC as shown in Figure 4-6. It is only necessary to load this buffer once every frame.

After the X- and Y-buffers of MULACC are loaded, the following filtering operation is implemented for each subband:

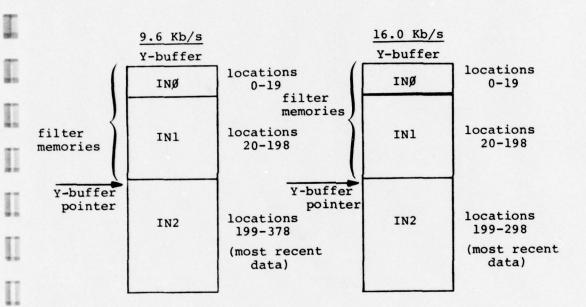


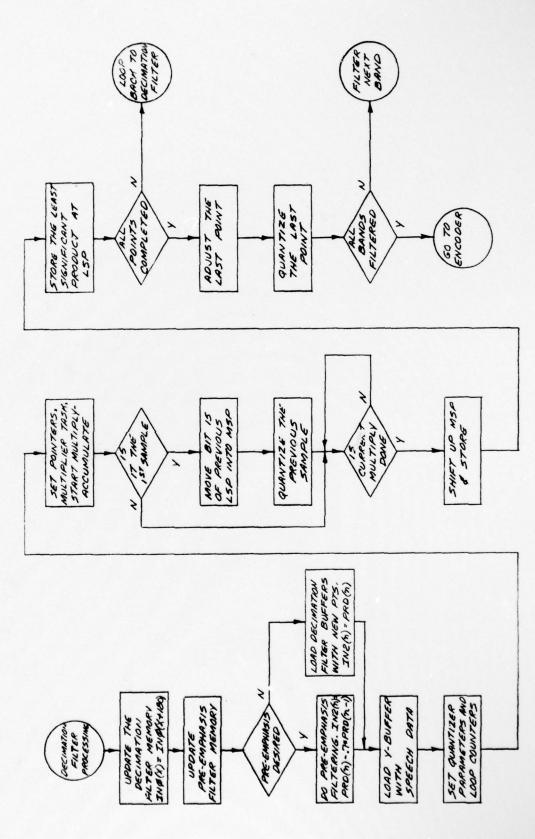
FIGURE 4-6 LOADING OF THE Y-BUFFER FOR DECIMATION FILTERING

$$y(nL) = \sum_{k=0}^{199} h(k)x(nL-k)$$
 (4-1)

where L is the decimation ratio, h(k) is the kth filter coefficient, $x(\cdot)$ is the input sample, and $y(\cdot)$ is the filtered output

Initially, MULACC is setup to perform multiply and accumulate with no rounding; increment X-buffer and decrement Y-buffer pointers. The X-buffer pointer is directed to the first filter coefficient, h(0), of band 1 and the Y-buffer one is set to point at x(0) which is stored at the 199th location of the Y-buffer. By setting the loop counter to be equal to 200, the filtering operation is started. After MULACC finishes, the ready bit in the extended product (XTP) is set and the result is transferred to PSP. Incrementing the Y-pointer by a factor of L and resetting the X-pointer to & computation of the second sample is performed. Since it takes MULACC 42 msec to compute each output the PSP is free to perform other functions. In the point, real-time programs, this time is used for the quantization of the previously computed sample, thereby hiding the amount of time needed for quantization.

When the point y(nL) is computed, the X and Y buffer pointers are reset to compute the point y((n+1)L). If all the points for the particular band have been calculated, program control is transferred to the filter loop of the next subband. Once the filtering for all bands is complete, the program leaves for the encoder routine. Figure 4-7 is a flow chart that describes the operation of the decimation filters for the 9.6 Kb/s system. The corresponding codes for the 16.0 Kb/s system are similar.



I

I

I

4.6 Quantization and Encoding

After the band-pass filtering and decimation operations, the resulting subband signals are converted to binary bit streams using adaptive PCM (APCM) quantizers. Employing the adaptation strategy of one-word memory, the quantizer dynamically adjusts its step sizes according to the amplitude of the input signal. Maximum and minimum step sizes, adaptation and gain factors for the quantizers are summarized in Table 2-3. As described earlier, the quantization is done within the subband filtering loop in the program to minimize processing time.

Since the adaptive quantizer is known to perform poorly in the presence of channel errors, the robust algorithm as described in Appendix D is incorporated. In the actual implementation, the decaying factor β is chosen to be 0.96 and the function Δ^{β} , where Δ is the quantizer step-size, is estimated using a polynomial approximation procedure as described in Appendix E. To further reduce processing time, only a 3rd order polynomial is utilized. The flow-chart of an 8-level, robust quantizer is shown in Figure 4-8.

After quantizing the subband signals, the resulting bit stream is encoded and stored in the appropriate output buffer as depicted in Figure 4-9. The formats of the transmission data for both 9.6 and 16.0 Kb/s are shown in Figures 4-10(a) and (b). Upon finishing the encoding process, all transmitter functions have been completed. Then a sync pulse is outputted to denote the end of all transmitter functions and program control is transferred back to the wait loop.

4.7 Decoding and Dequantization

When the receiver ready flag (LNSW) is set equal to 1, the program will leave the wait loop and go to the receiver code. Decoding of the received data as shown in Figure 4.11 is the first function performed. Through this procedure, the receiver reconstructs code words from the data buffer each of which corresponds to a transmitted sample.

After the decoding, dequantizer routines are employed to

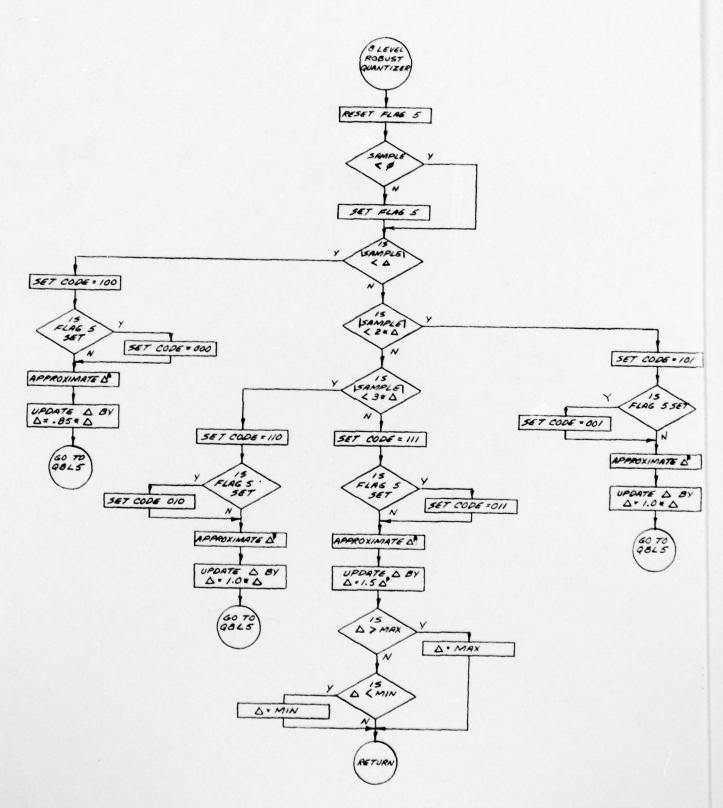
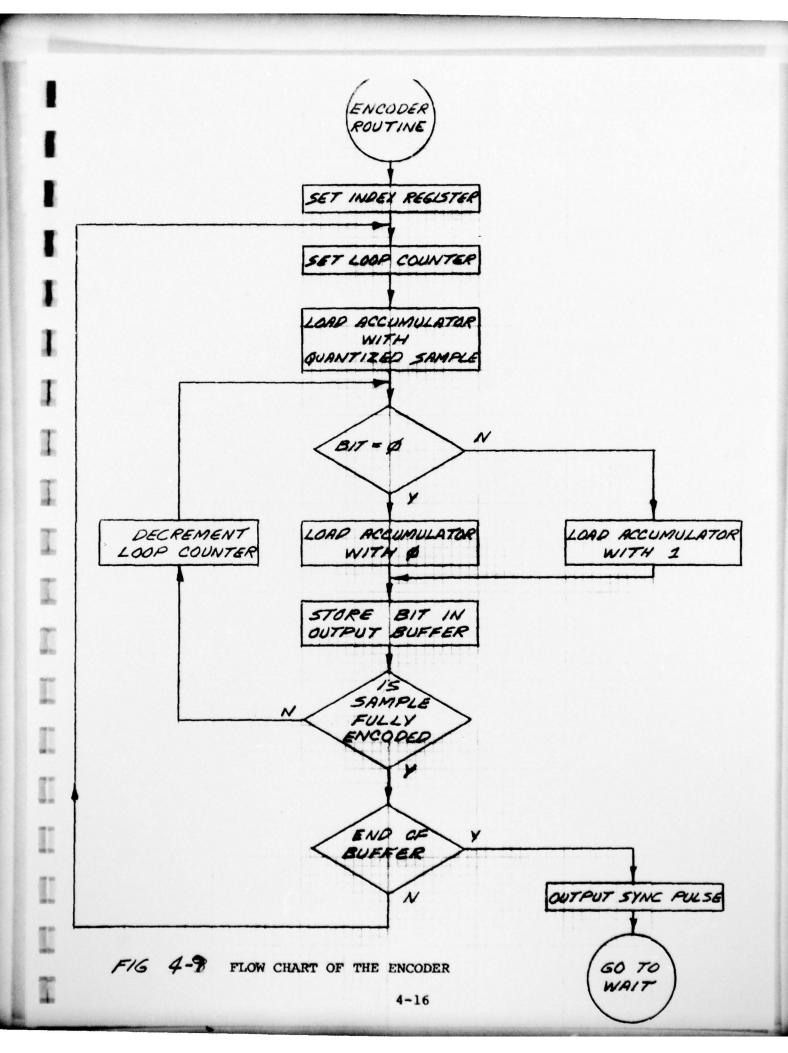


FIGURE 4-8 FLOW CHART OF AN 8-LEVEL ROBUST QUANTIZER



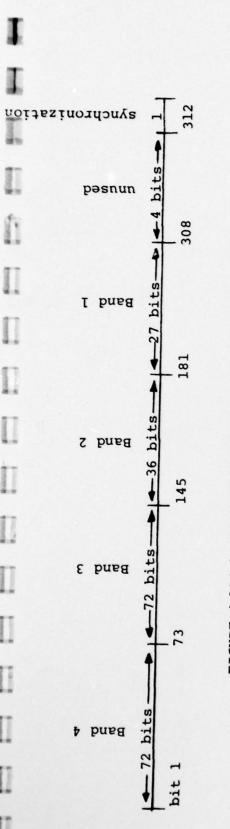


FIGURE 4-10(a) TRANSMISSION DATA FORMAT FOR 9.6 Kb/s

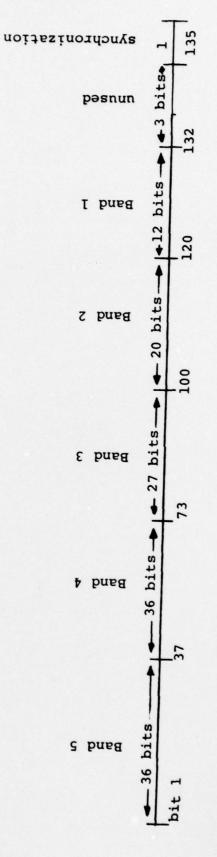
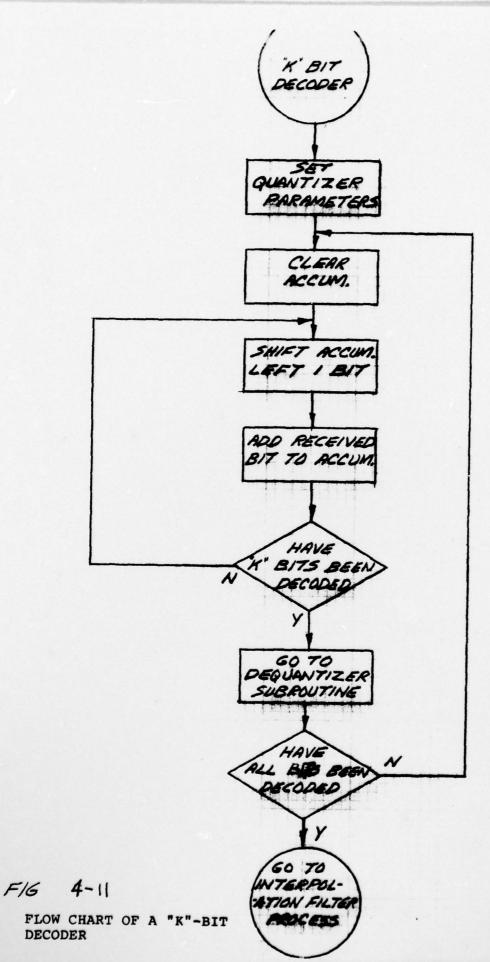


FIGURE 4-10(b) TRANSMISSION DATA FORMAT FOR 16.0 Kb/s



4-18

flow chart description of an 8-level wobust dequantizer is depicted in Figure 4-13. Whenever the dequantizer step size Δ falls below a pre-determined threshold value Δ th, a mid-rise/mid-tread switch, as described in Section 2, is used to eliminate the tones generated during idle channel conditions.

4.8 Interpolation Filtering

After dequantizing the received samples, they are stored in the approporate filter buffers. Since the received sample sequence contains information on the original signal only at intervals of L samples, where L is the decimation (interpolation) ratio, the remaining L-l samples are generated by interpolation filtering at the receiver as shown in Figure 4-13.

The real-time interpolation filter code implements the following:

$$y(n) = \sum_{k=0}^{199} h(k) x \left[\frac{n-k}{L} \right]$$
 (4-2)

where $\lceil \xi \rceil$ is defined as:

$$[\xi] = \begin{cases} \xi & \text{if } \xi \text{ is an integer} \\ 0 & \text{otherwise} \end{cases}$$
 (4-3)

As discussed in Section 2, it is not necessary to perform 200 multiplies to obtain each output sample owing to the fact that a lot of the input points $x(\cdot)$ are zero. For the sake of clarity, the following interpolations of Band 1 signal in the 9.6 Kb/s system are examined in detail (L=20):

$$y(0) = h(0) \times (0) + h(20) \times (-1) + \dots + h(180) \times (-9)$$

$$y(1) = h(1) \times (0) + h(21) \times (-1) + \dots + h(181) \times (-9)$$

$$\vdots$$

$$y(19) = h(19) \times (0) + h(39) \times (-1) + \dots + h(199) \times (-9)$$

$$y(20) = h(0) \times (1) + h(20) \times (0) + \dots + h(180) \times (-8)$$

$$y(21) = h(1) \times (1) + h(21) \times (0) + \dots + h(181) \times (-8)$$

$$\vdots$$

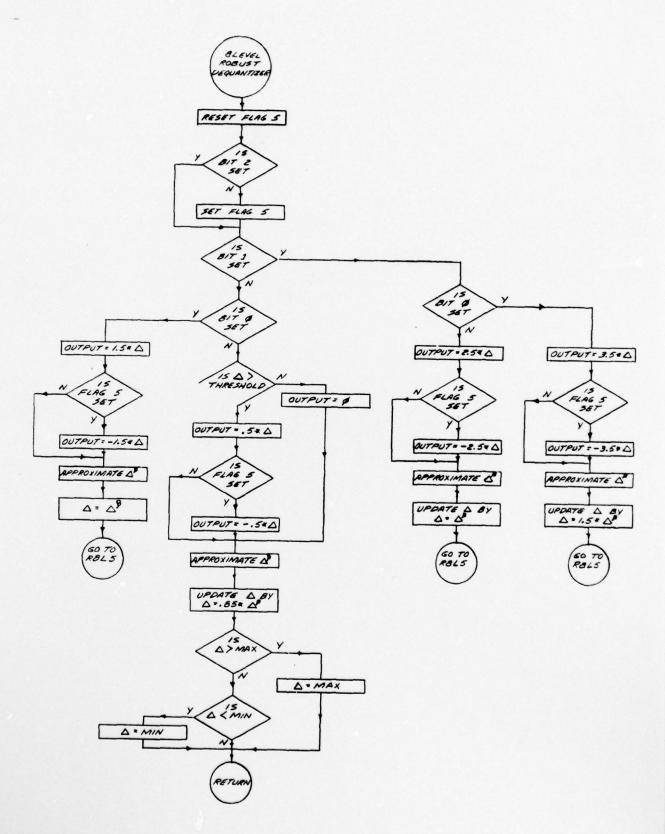


FIGURE 4-12 FLOW CHART FOR AN 8-LEVEL ROBUST DEQUANTIZER

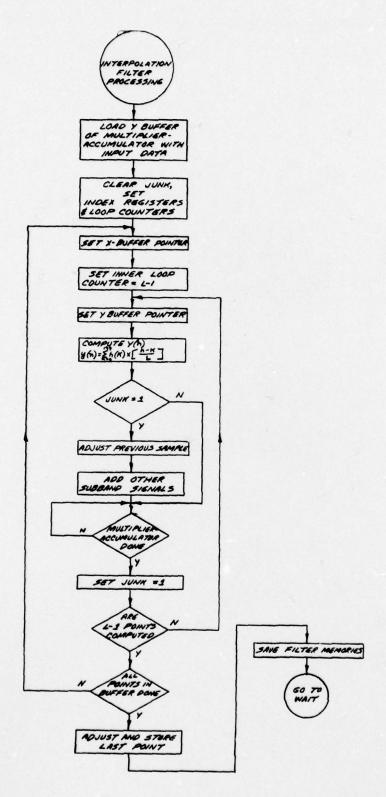


FIGURE 4-13 FLOW CHART FOR INTERPOLATION FILTERING

$$y(39) = h(19) \times (1) + h(39) \times (0) + ... + h(199) \times (-8)$$

$$\vdots$$

$$y(179) = h(19) \times (8) + h(39) \times (7) + ... + h(199) \times (-1)$$

It is obvious from the above equations that only 200/20 multiplications are needed to calculate each y(n). Furthermore, by arranging the filter coefficients and input samples in a special fashion, as shown in Figure 4-11, the output values can be efficiently computed using the MULACC.

Initially, the Y-buffer pointer is set to $X(\emptyset)$ and the X-buffer pointer is set to $h(\emptyset)$. The multiplier is set up to perform ten multiply-and-accumulates with both the X and Y pointers incrementing after each operation. When MULACC finishes, y(0) is computed. Then with the X-buffer pointer directing at h(1) and resetting the Y-buffer pointer to x(0), MULACC is restarted which later yields y(1).

The process is iterated for L-2 times and y(2), y(3) ... y(19) are computed. Then the X-buffer pointer is reset to h(0) and the Y-buffer pointer is set to x(1). By repeating the above procedure, all interpolator outputs are computed. Tallying up the multiplies involved, it is noted that the total number is roughly comparable in both interpolation and decimation filtering. However, a closer examination of the real-time implementation reveals that that symmetry of the FIR filters has not been exploited. This can be explained by the fact that programming of MULACC is more efficient when the filter coefficients are strung out. Furthermore, the speed of MULACC is capable of performing full-duplex 9.6 Kb/s subband coder and the more complicated 16.0 Kb/s system in a half-duplex mode.

When interpolation filterings for all subbands are finished, the resulting points are added together before being loaded into the output buffer. Then a sync pulse is generated to signify the end of the receiver function and the program returns to the wait loop.

X-buffer		Y-buffer	
	h(0)		X (79)
	h(20)		:
	h(40)		X(6)
			X(5)
			X(4)
	h(180)		X(3)
	h(1)		X(2)
	h(21)		X(1)
	h(41)		X(0)
			x(-1)
	h(181)		X (-2)
			X(-3)
			X(-4)
	h(19)		X(-5)
	h(39)	1	X(-6)
			X(-7)
			X(-8)
	h(199)		X(-9)

1

FIGURE 4-14 STORAGE OF X AND Y-BUFFERS FOR INTERPOLATION FILTERING

4.9 Operating Procedures of the Real-Time Subband Coder Programs

4.9.1 9.6 Kb/s Program

I. LOADING

Load the program SBC96.PBJ into both PSP's using the PSP Loader Program PSPLD.

II. OPERATING PROCEDURES

After the program has been loaded, depress bit 15 of PSP front panel switches. Then start the subband coder program by setting the RUN/STOP switch to RUN. In this mode, the program will loop around an initialization routine which clears out data buffers and resets loop registers. When bit 15 is placed in the up position, the software will first enable synchronization between the two PSP's and then proceed to process speech using the subband coder algorithm. If re-synchronization is desired, hold bit 15 of both PSP's in the down position and return it one at a time to the up position. Options of the 9.6 Kb/s subband coder program are summarized as:

bit 15 DOWN: INITIALIZATION

UP: NORMAL OPERATION

bit 12 DOWN: ROBUST QUANTIZER

UP: ADAPTIVE JAYANT QUANTIZER

4.9.2 16.0 Kb/s Program

I. LOADING

Load the program SBCl6.PBJ into both PSP's using the PSP Loader Program PSPLD.

II. OPERATING PROCEDURES

bit 12

After the program has been loaded, depress bit 15 of PSP front panel switches. Then start the subband coder program by setting the RUN/STOP switch to RUN. In this mode, the program will loop around an initialization routine which clears out data buffers and resets loop registers. When bit 15 is placed in the up position, the software will first enable synchronization between the two PSP's and then proceed to process speech using the subband coder algorithm. If re-synchronization is desired, hold bit 15 of both PSP's in the down position and return it to the up position. Since the 16 Kb/s subband coder program only works in the half-duplex mode, the push-to-talk switch on the handset has to be depressed to allow speech transmission. Options of the 16.0 Kb/s subband coder program are summarized as:

bit	15	DOWN:	INITIALIZATION
		UP:	NORMAL OPERATION
bit	14	DOWN:	TRANSMITTER
		UP:	PUSH-TO-TALK
bit	13	DOWN:	RECEIVER
		UP:	PUSH-TO-TALK

DOWN:

UP:

ROBUST QUANTIZER

ADAPTIVE JAYANT QUANTIZER

SECTION V

Conclusions and Recommendations

5.1 Conclusions

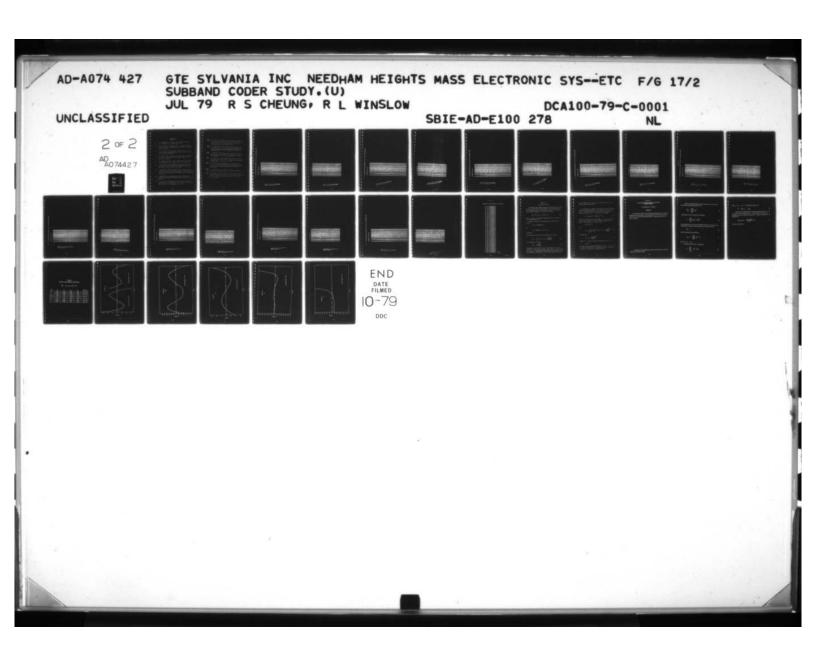
This contract has resulted in the development of a 9.6 and a 16.0 Kb/s real-time subband coder which employ the integer-band sampling technique. Informal listening tests indicate that the speech quality of the subband coders is slightly "hollow" and noisy especially for the 9.6 Kb/s system, but its overall quality is significantly better than that of CVSD at the same data rate. However, when compared to other high quality 16 Kb/s speech encoding schemes, such as the Adaptive Predictive Coder with Adaptive Quantization (APCQ), the subband coder is clearly inferior. GTE Sylvania attributes this to the fact that the four or five bandpass filters employed by the subband coder algorithm are not adequate to represent the entire speech spectrum. introduces spectral "gaps" which manifest the "hollowness" in the processed speech. Moreover, the ratio of subband energies fluctuates largely from frame to frame and quantization of them using adaptive PCM (APCM) with fixed bit allocations results in noisier output speech.

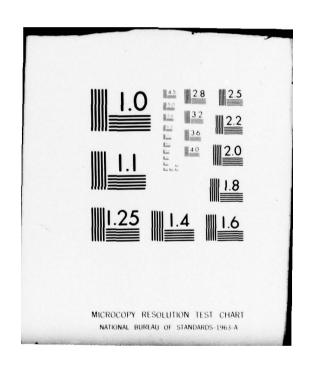
In light of the inadequacy of the integer-band sampling approach, GTE Sylvania developed an improved subband coding scheme using quadrature mirror filters (QMF). An adaptive bit allocation scheme is also incorporated to quantize the subband signals. FORTRAN simulations show that no significant distortions are introduced in the bandsplitting/reconstruction process using QMF filters and this results in "smoother" quality processed speech. Furthermore, the adaptative bit allocation scheme enables a more efficient encoding of the subband waveforms which eliminates a lot of quantization noise in the outputs speech.

5.2 Recommendations

Encouraged by the latest results, GTE Sylvania strongly recommends the subband coding algorithm with the QMF approach be studied further and be implemented especially at 16 Kb/s. More-

over, since present subband coders are only designed to capture the spectral shape of the speech signal, GTE Sylvania believes that the speech quality of the QMF method can be further improved by exploiting the fine structures of the speech spectrum. This is also reinforced by the findings of a recent study which incorporates pitch information in performing subband coding of speech signals [14].





REFERENCES

- [1] J. L. Flanagan et al, "Speech Coding," IEEE Trans Comm., Vol. COM-27, No. 4, pp 710-736, Apr., 1979.
- [2] R. E. Crochiere, S. A. Webber and J. L. Flanagan, "Digital Coding of Speech in Subbands," Bell Syst. Tech. J., Vol. 55, No. 8, Oct., 1976.
- [3] R. E. Crochiere, "On the Design of Subband Coders for Low Bit-Rate Speech Communication," Bell Syst. Tech. J., Vol. 56, No. 5, pp 747-770, May 1977.
- [4] R. W. Shafer and L. R. Rabiner, "A Digital Signal Processing Approach to Interpolation," Proceedings of IEEE, Vol. 61, pp 692-702, June 1973.
- [5] N. S. Jayant, "Digital Coding of Speech Waveform: PCM, DPCM and DM Quantizers," Proc. IEEE, Vol. 62, No. 5, May 1974.
- [6] R. E. Crochiere, "A Mid-Rise/Mid-Tread Quantizer Switch for Improved Idle-Channel Performance in Adaptive Coders," Bell Syst. Tech. J., Vol. 56, No. 9, Oct. 1978.
- [7] D. Esteban and C. Galand, "Applications of Quadrature Mirror Filters to Split Band Voice Coding Schemes," IEEE International Conference on Acoustics, Speech and Signal Processing, Hartford, Conn., 1977.
- [8] O. Hermann, "On the Approximation Problem in Nonrecursive Digital Filter Design," IEEE Trans. Circuit Theory, Vol. CT-18, May 1971.

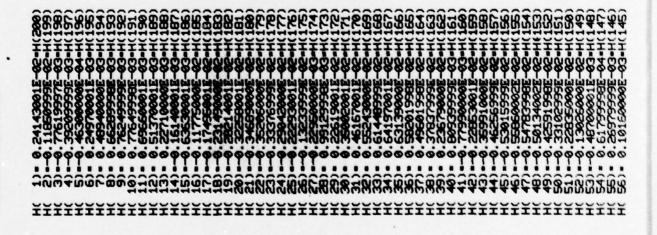
1

[9] L. E. Bergeron, "A Maximally Flat Filter Design Algorithm for Quadrature Mirror Filters," Conf. Rec. IEEE Int. Conf. Acoust., Speech and Sig. Proc., Washington, D.C., 1979.

- [10] A. Crosier, D. Esteban and C. Galand, "Perfect Channel Splitting by Use of Interpolation/Decimation/Tree Decomposition Techniques," 1976 International Conference on Information Sciences and Systems, Patras.
- D. Esteban and C. Galand, "32 KBPS CCITT Compatible Split-Band Coding Scheme," Conf. Record of IEEE International Conference Acoustics, Speech and Signal Processing, Tulsa, OK, April 1978.
- J. Huang and P. Schultheiss, "Block Quantization of Cor-Related Gaussian Random Variables," <u>IEEE Trans. Communications Systems</u>, Vol. CS-11, 1963, pp 289-296.
- R. Zelinski and P. Noll, "Approaches to Adaptive Transform Speech Coding at Low Bit Rates," <u>IEEE Trans. Acoust. Speech and Sig. Proc.</u>, Vol. ASSP-27, Feb. 1979.
- R. E. Crochiere, "A New Approach for Implementing Pitch Prediction in Subband Coding," Conf. Rec. IEEE International Conf. on Acoust., Speech and Sig. Proc., Washington, D.C., April 1979.
- [15] D. J. Goodman and R. M. Wilkinson, "A Robust Quantizer,"
 IEEE Trans. on Communications, Vol. COM-23, No. 11, Nov. 1975.
- H. G. Martinez and T. W. Parks, "A Class of Infinite-Duration Impulse Response Digital Filters for Sampling Rate Reduction," IEEE Trans. Acoust., Speech and Sig. Proc., Vol. ASSP-27, No. 2, April 1979.

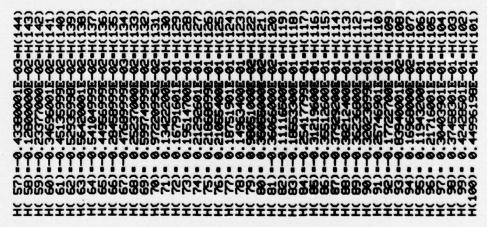
1

APENULK A



THIS PAGE IS BEST QUALITY PRACTICALISMS

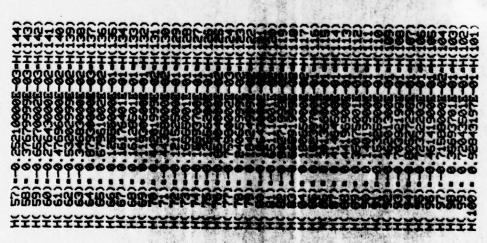
A.1 (cont'd)



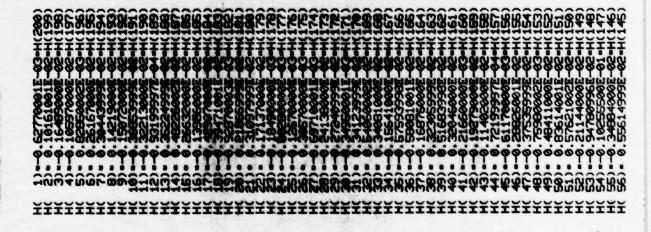
THIS PAGE IS BEST QUALITY PRACTICABLE FROM GOPY FURNISHED TO DDC

THIS PAGE IS BEST QUALITY PRACTICABLE FROM GOPY FUMPLISHED TO DDC

A.2 (cont'd)



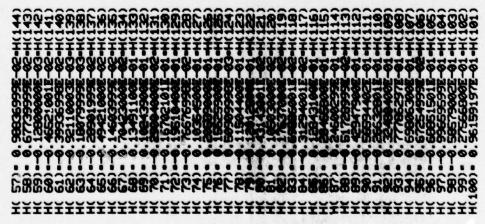
THIS PAGE IS BEST QUALITY PRACTICALLY FROM GOVY PARALSHED TO DOG



THIS PAGE IS BEST QUALITY PRAGRICARUM FROM GOPY PURPHISHED TO DDC

A.3 (cont'd)

1



THE S PACK IS BEST QUALITY FRANCISMENT IN THE PACK IN BUSINESS OF THE PACK IN THE PACK IN

. 4 FILTER COEFFICIENTS FOR BAND 4 OF THE 9.6 KB-S SUB-BAND CODER

FILENATE IS F4.NM

```
| Colored | Colo
```

THIS PAGE IS BEST QUALITY PRACTICABLE FROM GOPY FUNDISHED TO DDC

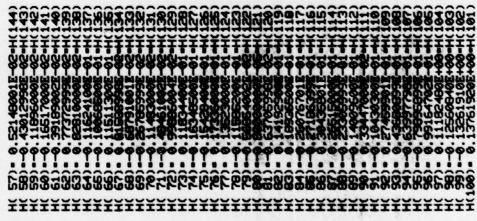
A.4 (cont'd)

.

I

I

I



THIS PAGE IS BEST QUALITY PRACTICABLE FROM GOPY FURNISHED TO DDC APPENDIX B

FILTER COEFFICIENTS FOR BAND 1 OF THE 16. KB/S SUB-BAND CODER

B.1

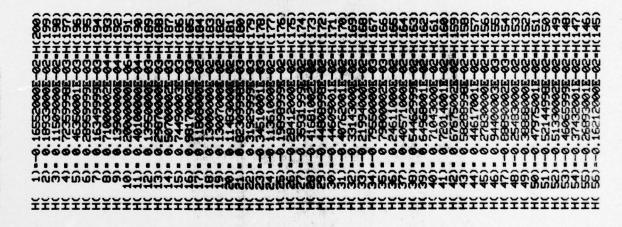
FILENOME IS FILTI. NAM

| Colored | Colo

THIS PAGE IS BEST QUALITY PRACTICABLE FROM GOFY FURNISHED TO DDC

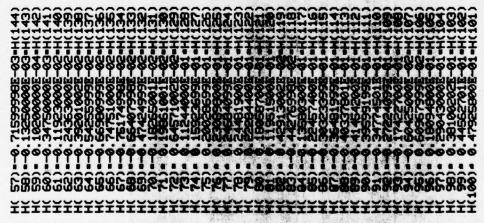
(cont'd)

THIS PACE IS BEST QUALITY PRACTICABLE FROM CUTY FURNISHED TO DDC



THIS PAGE IS BEST QUALITY PRACTICABLE FROM GOPY PURMISHED TO DDC

B.2 (cont'd)



I Hade so

THIS PAGE IS BEST QUALITY PRACTICABLE FROM GOPY FURNISHED TO DDC

Π

П

88888888888888888888888888888888888888	1
~~~~~~~~~~~~~~~~~~~~~~~~~~~~~~~~~~~~~~	
11120000000000000000000000000000000000	
<b>෪෧෧෧෧෧෧෧෧෧෧෧෧෧෧෧෧෧෧෧෧෧෧෧෧෧෧෧෧෧෧෧෧෧෧෧෧</b>	3
**************************************	:

THIS PAGE IS BEST QUALITY PRACTICABLE

FROM COPY *: *** ISHED TO DDC

(cont'd)

THIS PAGE IS BEST QUALITY PRACTICABLE FROM GOPY PAREISHED TO DDC I

THIS PAGE IS BEST QUALITY PRACTICABLE FROM COPY PURBISHED TO DDC

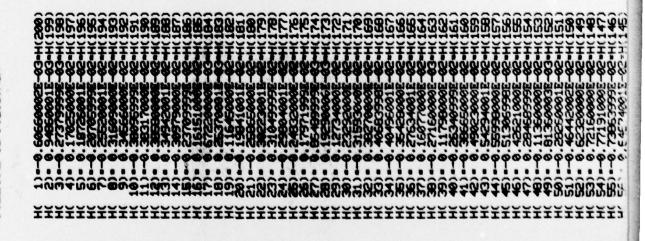
I

1

I

THIS PAGE IS BEST QUALITY PRACTICABLE TROM GOPY PURPLISHED TO DDC

Tomas .



THIS PAGE IS BEST QUALITY PRACTICABLE FROM GOPY PUREISHED TO DOC

B.5 

THE PLOK IS BEST QUALITY PRACTICABLE FROM GOPY FURNISHED TO DOC

#### APPENDIX C

## TABULATION OF THE 60-TAP QMF IMPULSE RESPONSE

```
1)=-0.80456801E-10
2)=-0.12466006E-08
H(
    3)= 0.33937912E-08
    4)= 0.12555994E-07
    5)=-0.54866284E-07
H(
    6)=-0.79773159E-07
    7)= 0.56410033E-06
H(
    8) = 0.19332403E-06
    9)=-0.40112018E-05
HC
H( 10)= 0.13859838E-05
H( 11)= 0.20943698E-04
H( 12)=-0.18127259E-04
H( 13)=-0.83554602E-04
H( 14)= 0.11246781E-03
H( 15)= 0.26012788E-03
H(16) = -0.49234246E - 03
H( 17)=-0.63178962E-03
H(18) = 0.16880841E-02
H( 19)= 0.11479852E-02
H( 20)=-0.47692582E-02
H( 21)=-0.12668951E-02
H( 22)= 0.11493831E-01
H(23) = -0.66263479E - 03
H( 24)=-0.24424994E-01
H( 25)= 0.84577305E-02
H( 26)= 0.48056692E-01
H( 27)=-0.31792097E-01
H( 28)=-0.98794423E-01
H( 29)= 0.12183660E+00
H( 30)= 0.46986365E+00
H( 31)= 0.46986365E+00
H( 32)= 0.12183660E+00
H(33) = -0.98794423E - 01
H(34) = -0.31792097E - 01
H(35) = 0.48056692E-01
H( 36)= 0.84577305E-02
H(37) = -0.24424994E - 01
H(38) = -0.66263479E - 03
H( 39)= 0.11493831E-01
H( 40)=-0.12668951E-02
H( 41)=-0.47692582E-02
H( 42)= 0.11479852E-02
H(43) = 0.16880841E-02
H( 44)=-0.63178962E-03
H( 45)=-0.49234246E-03
H( 46)= 0.26012788E-03
H( 47)= 0.11246781E-03
H( 48)=-0.83554602E-04
H( 49)=-0.18127259E-04
H( 50)= 0.20943698E-04
H( 51)= 0.13859838E-05
H( 52)=-0.40112018E-05
H( 53)= 0.19332403E-06
H( 54)= 0.56410033E-06
H( 55)=-0.79773159E-07
H( 56)=-0.54866284E-07
H( 57)= 0.12555994E-07
H( 58) = 0.33937912E-08
H(59) = -0.12466006E - 08
H( 60)=-0.80456801E-10
```

659-79

## Appendix D

#### The Robust Quantizer

The subband coder employs adaptive PCM (APCM) quantizers with the Jayant algorithm which performs well in a back-to-back mode without channel errors. Unfortunately, channel errors significantly impair performance. To see this, consider

$$q_k = M(I_k) q_{k-1} = \frac{k}{m} M(I_i) q_0$$
 (D-1)

where  $I_i$  is the ith transmitted character and  $M(I_i)$  is the multiplier corresponding to  $I_i$ .

Assume now that one transmission error is made at time  $\ell$  causing

$$M(I_{\varrho})$$
 to become  $M(I_{\varrho}')$ 

and

$$q_{\ell}$$
 to become  $q_{\ell}' = M(I_{\ell}') q_{\ell-1}$ 

afterwards,

the new quantizer levels for time greater than  $\ell$  become

$$q_{k}' = \frac{k}{m} M(I_{i}) M(I_{\ell}') q_{0} \cdot \left[\frac{M(I_{\ell})}{M(I_{\ell})}\right] \qquad (D-2)$$

or, simplifying, we obtain

$$q_{k'} = q_{k} \frac{M(I_{\ell'})}{M(I_{\ell})}$$
 (D-3)

Consequently, the effects of even a single-channel error never die out. In fact, an error causes a level shift in  $\mathbf{q}_k$  by the factor  $M(\mathbf{I}_{\ell}')/M(\mathbf{I}_{\ell})$ . Simulations show that errors cause noticeable fades and increases in output level. Only when the quantizer saturates

at its maximum level or cuts off at its minimum level does the quantizer again track properly.

By incorporating a small decaying factor in the Jayant algorithm, the resulting quantizer can be made more robust to channel errors. This modification calls for the raising of the last quantizer step size,  $q_{k-1}$ , to a power  $\beta$  as follows [15]

$$q_k = M(I_k) q_{k-1}^{\beta} = \frac{k}{\pi} M(I_i)^{\beta k-1} q_0$$
 (D-4)

where  $\pi(\cdot)$  represents the product symbol,  $I_i$  is the ith transmitted symbol, and  $M(I_i)$  is the multiplier corresponding to  $I_i$ . Again, if one channel error occurs at time  $\ell$ 

$$M(I_0) \rightarrow M(I_0')$$

and

I

$$q_{k'} = \prod_{\substack{i=1\\i=\ell}}^{k} \left[ M(I_{i}) \right]^{\beta k-i} M(I_{\ell'})^{\beta k-\ell} q_{0} \cdot \left[ \frac{M(I_{\ell})^{\beta}}{M(I_{\ell})^{\beta}} \right]^{\beta k-\ell}$$
(D-5)

or simplifying

$$q_{k'} = q_{k} \cdot \left[\frac{M(I_{\ell'})}{M(I_{\ell})}\right]^{q_{k}}$$
 (D-6)

Assuming  $\beta$  < 1, then for times k far removed from  $\ell$  (k >>  $\ell$ ),

$$q_k' + q_k$$

The speed of this convergence depends on how near  $\beta$  is to 1. If  $\beta$  is not too close to unity, convergence is rapid. Consequently, the effect of a single error decays with time.

#### APPENDIX E

# EVALUATING TRANSCENDENTAL FUNCTIONS WITHOUT DIVISION

# A. Arcese and A. J. Goldberg

## **ABSTRACT**

We consider least square-error polynomial approximations to trancendental functions over a finite interval. These approximations are useful when computer division times greatly exceed multiplication times. Examples are given for 1/x,  $\sqrt{x}$ ,  $e^{-x}$ , and  $\ln x$ .

The authors are with GTE Sylvania, Electronics Systems Group, Needham Heights, Massachusetts, 02194.

Given a trancendental function f(x) over some interval (a,b), we seek an m; the degree polynomial approximation to f(x)

$$\widehat{f}(x) = \sum_{k=0}^{k=m} a_k x^k$$
 (1)

that minimizes the sum of squares of the residuals

$$J = \sum_{i=1}^{i=n} \left( f(x_i) - \widehat{f}(x_i) \right)^2$$
 (2)

over the interval (a,b). The  $x_i$  are the n sample data points in the interval (a,b). Minimizing J with respect to each coefficient  $a_k$ , we obtain the equation

$$\mathbf{R}\alpha = \gamma \tag{3}$$

where the elements of the matrix R are

$$||R|| = ||\sum_{k=1}^{k=n} x_k^{i+j-2}||$$
 (4)

where i, j = 1, 2, ..., m+1.

The right hand side vector  $\gamma$  has elements

$$\gamma_i = \sum_{k=1}^{k=n} x_k^{i-1} f(x_k)$$
 (5)

where i = 1, 2, ..., m+1.  $\alpha$  is the solution column vector

$$a^{T} = \begin{bmatrix} a_0, a_1, \dots, a_m \end{bmatrix}$$
 (6)

Table I gives the coefficients for a third degree approximation to 1/x,  $\sqrt{x}$ ,  $e^{-x}$ , and  $\ln x$  over the interval (0.5, 1.0). For 1/x and  $\ln x$  it was necessary to subdivide the interval to lower the maximum error. Figures 1 through 5 give the percent error

percent error = 
$$\left(\frac{f(x) - \widehat{f}(x)}{f(x)}\right) \times 100$$
 (7)

for each of the functions.

TABLE I
TABLE OF LEAST SQUARE COEFFICIENTS

$$\hat{f}(x) = a_0 + a_1 x + a_2 x^2 + a_3 x^3$$

f(x)	a ₀	a ₁	a ₂	a ₃	Range of x
1/x	4.895	-7.918	4.233	0.000	(0.5, 0.75)
	2.626	-1.081	-1.816	1.273	(0.75, 1.0)
√x	0.2613	1.116	-0.5193	0.1423	(0.5, 1.0)
e ^{-x}	1.060	-1.238	0.7905	-0.2451	(0.5, 1.0)
ln x	-2.222	4.392	-3.167	1.000	(0.5, 0.95)
	-1.007	0.4711	1.071	-0.5358	(0.95, 1.0)

